Manipulation of Biologically Important Structures Using the "End-to-End Distance Change" of Azobenzene Photoswitches

2020/6/8
Literature Seminar
Mina Yamane (M1)

Table of Contents

Table of Contents

Introduction

Azobenzenes

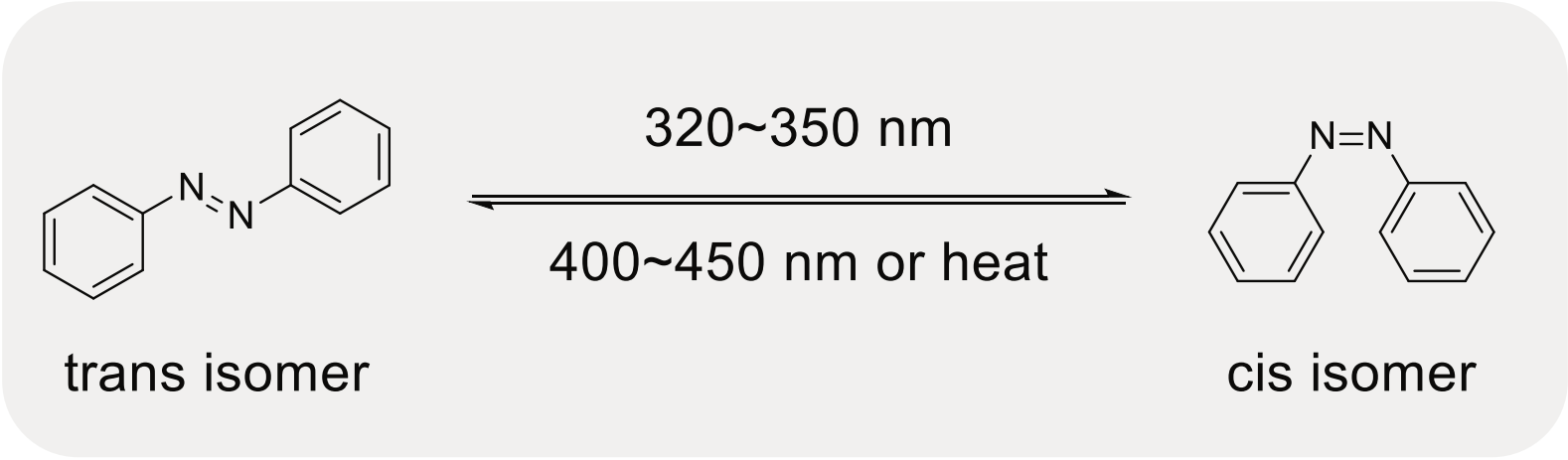

- ✓ *trans* isomer: near-planar, dipole moment ~0
- ✓ *cis* isomer: bent conformation, dipole moment~3 Debye
- ✓ stability: *trans* > *cis* (by 10~12 kcal mol^{-1})
- ✓ photoisomerization (picoseconds) vs. thermal relaxation (ms to days)
- ✓ end to end distance change: ~3.5 Å

A. Woolley *et al. Chem. Soc. Rev.* **2011**, *40*, 4422.
E. Merino *et al. Beilstein J. Org. Chem.* **2012**, *8*, 1071.

Photoisomerization Mechanisms

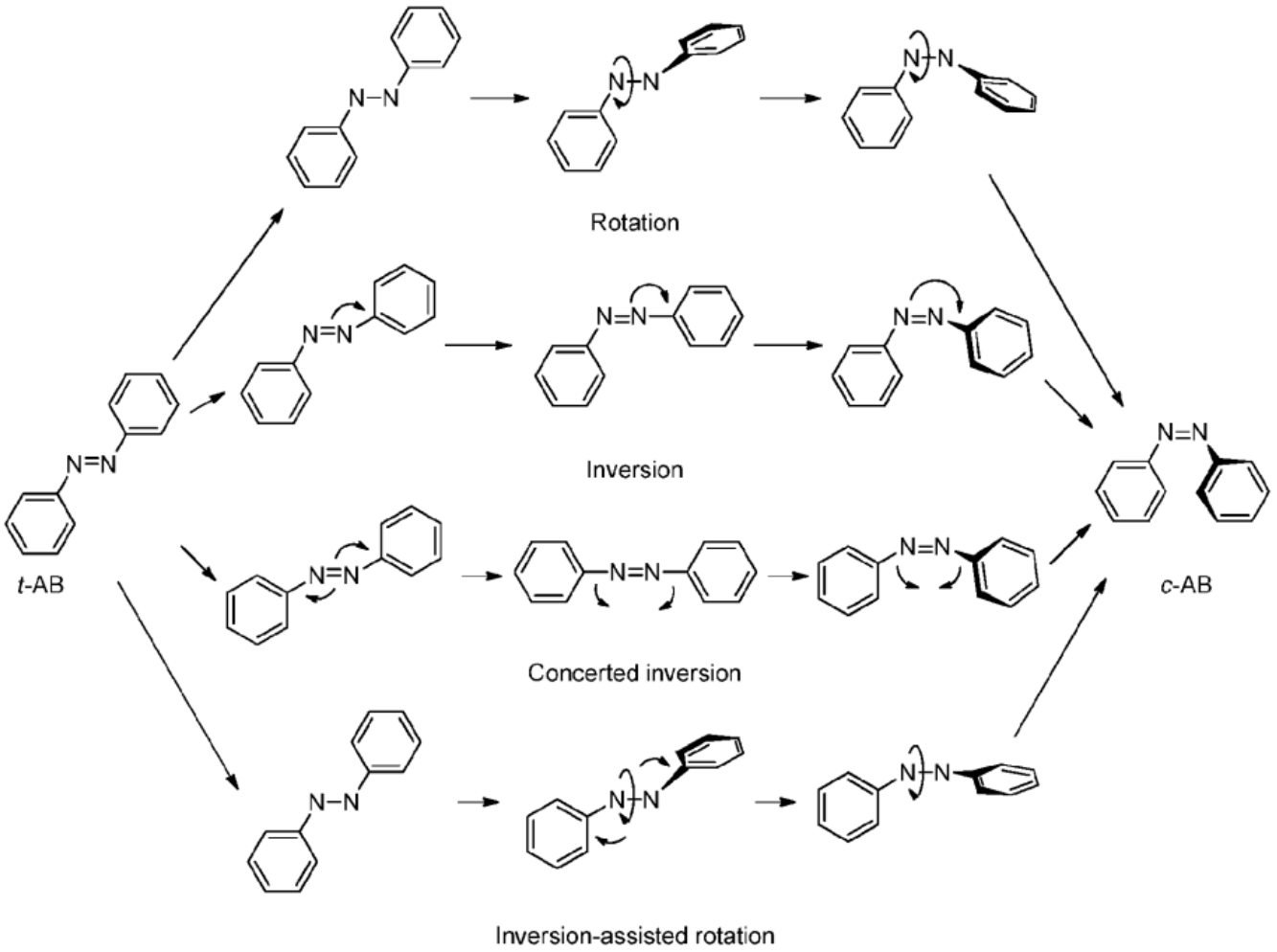

Scheme 1 Proposed mechanisms for the *trans* → *cis* isomerization of AB.

S. Burdette *et al. Chem. Soc. Rev.* **2012**, *41*, 1809.

A Brief History of Azobenzene

1834 — 1st description (Mitscherlich)

1937 — Discovery of photoisomerization (Hartley)

Application to polypeptides (Goodman) 1966

1981 — 1st light-driven molecular machines (Shinkai, Manabe)

2000

t

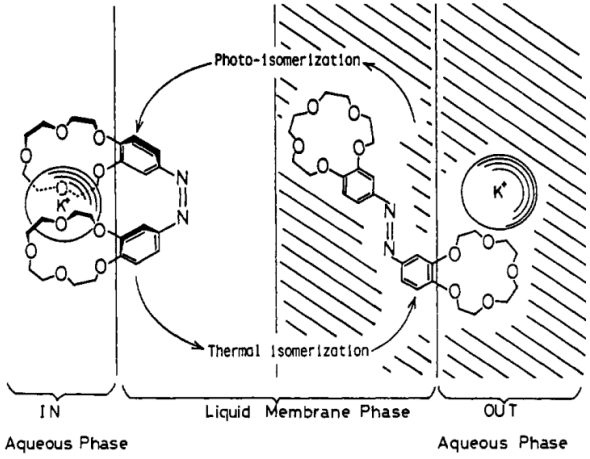

Figure 5. Schematic representation of light-driven ion transport.

"Phototweezers"

S. Shinkai, O. Manabe *et al. J. Am. Chem. Soc.* **1981**, *103*, 111.

A Brief History of Azobenzene

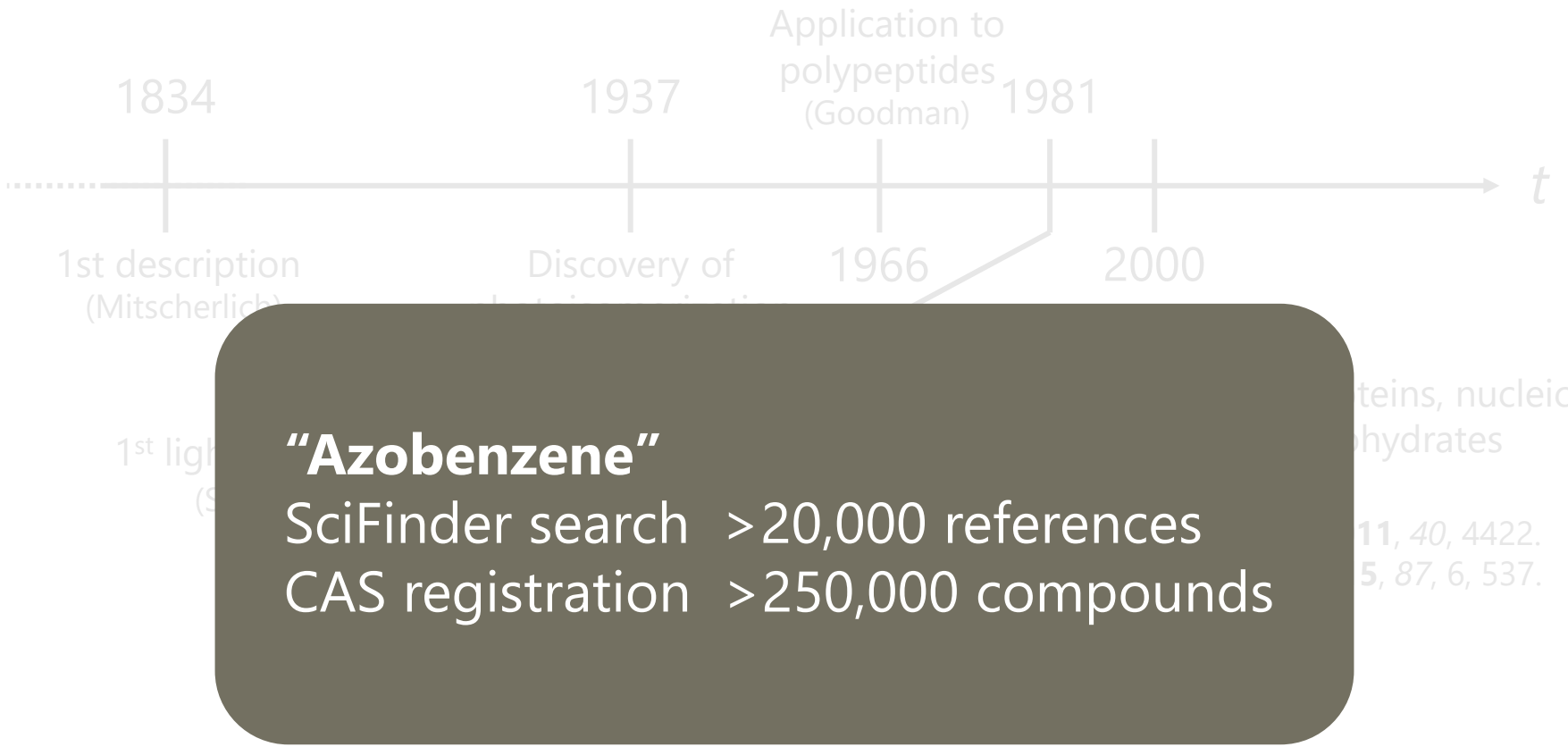

"Azobenzene"
SciFinder search >20,000 references
CAS registration >250,000 compounds

A. Credi *et al. Pure Appl. Chem.* **2015**, *87*, 6, 537.

A Brief History of Azobenzene

1834 — 1st description (Mitscherlich)

1937 — Discovery of photoisomerization (Hartley)

1966 — Application to polypeptides (Goodman)

1981 — 1st light-driven molecular machines (Shinkai, Manabe)

2000 — Wide application to biological systems

t

e.g.) peptides, proteins, nucleic acids, lipids, carbohydrates

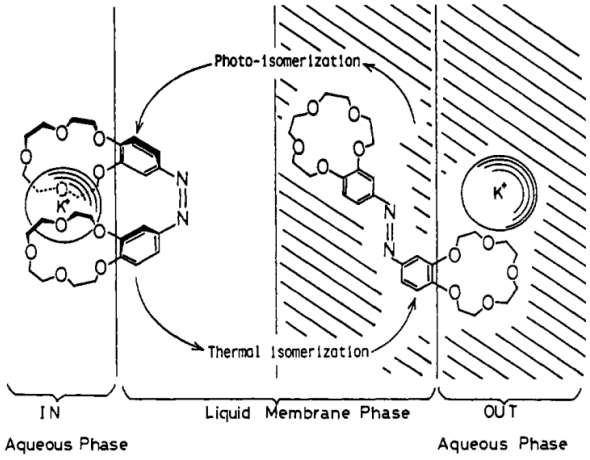

Figure 5. Schematic representation of light-driven ion transport.

"Phototweezers"

A. Woolley *et al. Chem. Soc. Rev.* **2011**, *40*, 4422.
A. Credi *et al. Pure Appl. Chem.* **2015**, *87*, 6, 537.

S. Shinkai, O. Manabe *et al. J. Am. Chem. Soc.* **1981**, *103*, 111.

Table of Contents

Photoswitches in Biomolecules

Table 1. Selected Molecular Structures of Photoswitches Introduced into Biomolecules

	Photoswitches	Isomerization	λ_1/λ_2	polarity change
A	Azobenzenes	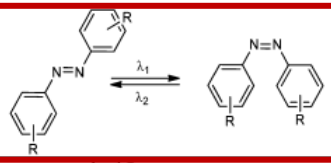	UV/VIS (ΔT)	medium (Δμ = ~3 D)
B	Stilbenes	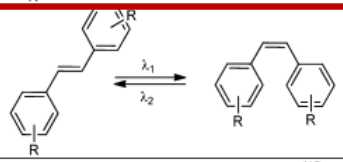	UV/UV	small
C	Spiropyrans	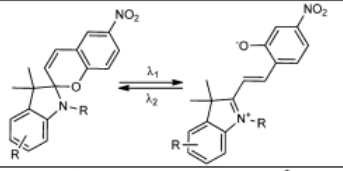	UV/VIS (ΔT) or VIS/UV	large (Δμ = 8-15 D)
D	Diarylethenes	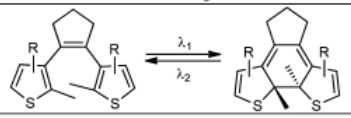	UV/VIS	small
E	Thiophenefulgides	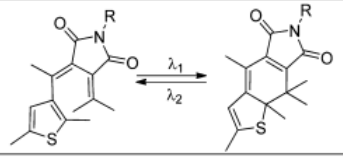	UV/VIS	small
F	Hemithioindigos	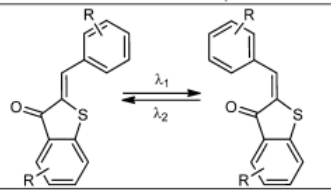	VIS/VIS (ΔT)	medium (Δμ = ~1.6 D)

Q. Why use azobenzenes?

A.

- ✓ Easy synthesis
- ✓ High photostationary states
- ✓ High quantum yields for transitions
- ✓ Fast photoisomerization (picosec)
- ✓ Minimal photobleaching

⇒ Effective molecular switch

B. Feringa *et al*. *Chem. Rev*. **2013**, *113*, 6114.
C. Renner and L. Moroder, **2006**, *7*, 868.

The "End-to-End" Distance Change

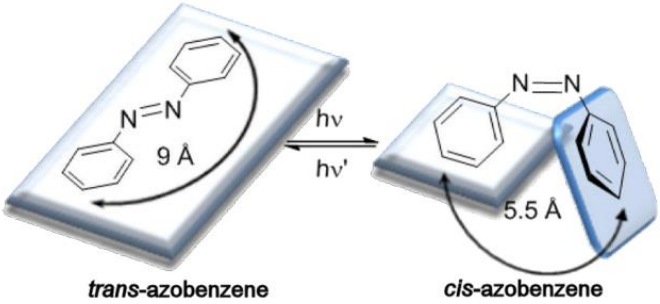

Figure 1: Photoisomerization process of azobenzene.

E. Merino *et al. Beilstein J. Org. Chem.* **2012**, *8*, 1071.

(Moroder *et al.*)

~13 Å (Standaert, Park)

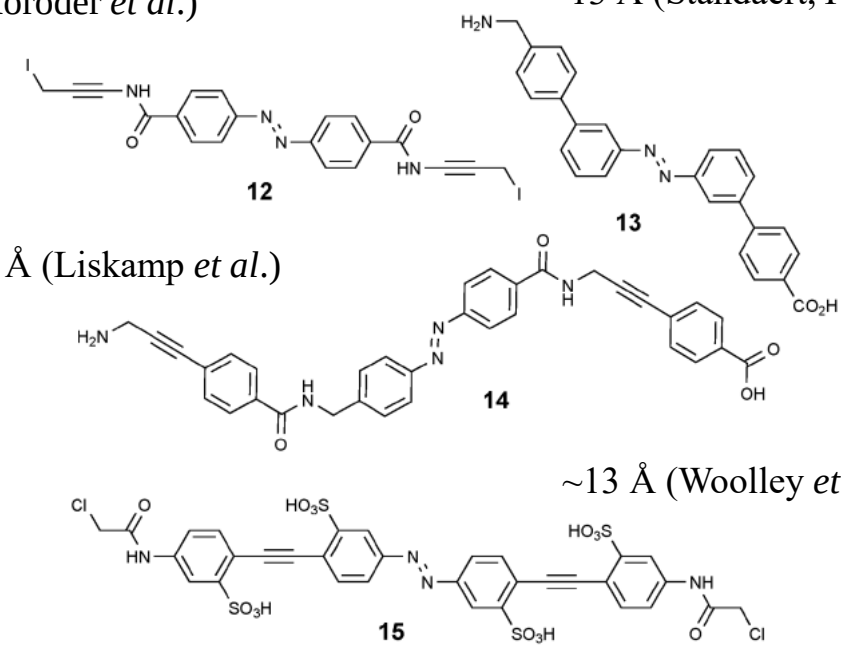

Fig. 3 Structures of some extended azobenzene-based photoswitches.

A. Woolley *et al. Chem. Soc. Rev.* **2011**, *40*, 4422.

⇒ The degree of functional change depends on the magnitude of the end-to-end distance change

Table of Contents

Strategies for Conformational Control

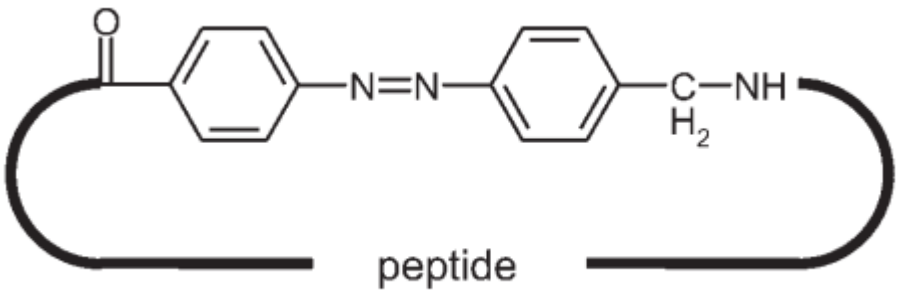

Backbone incorporation approach

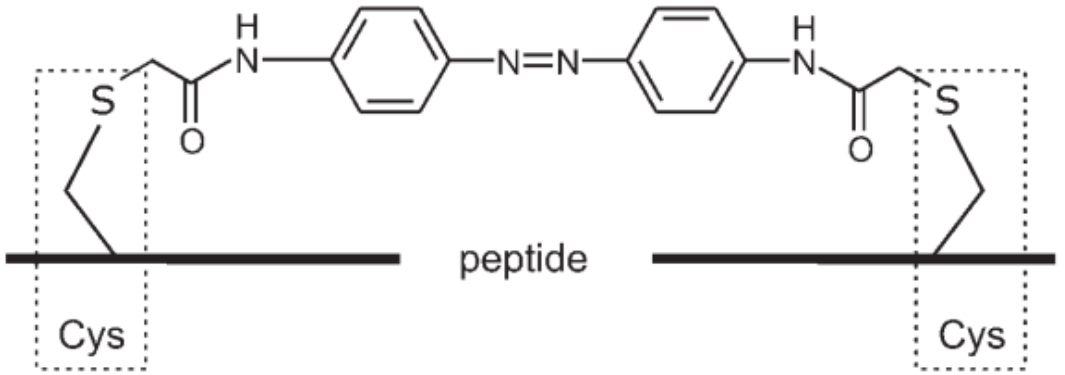

Side-chain Cross-link approach

Images from Scheme 2 of: C. Renner and L. Moroder, *ChemBioChem*. **2006**, *7*, 868.

Strategies for Conformational Control

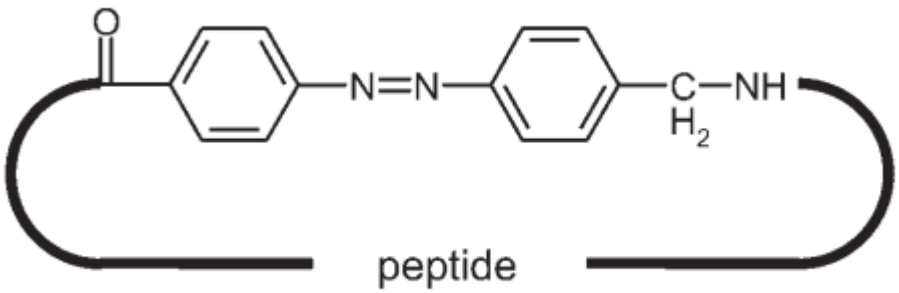

Backbone incorporation approach

Side-chain Cross-link approach

Images from Scheme 2 of: C. Renner and L. Moroder, *ChemBioChem*. **2006**, *7*, 868.

Example I. Backbone Incorporation Approach

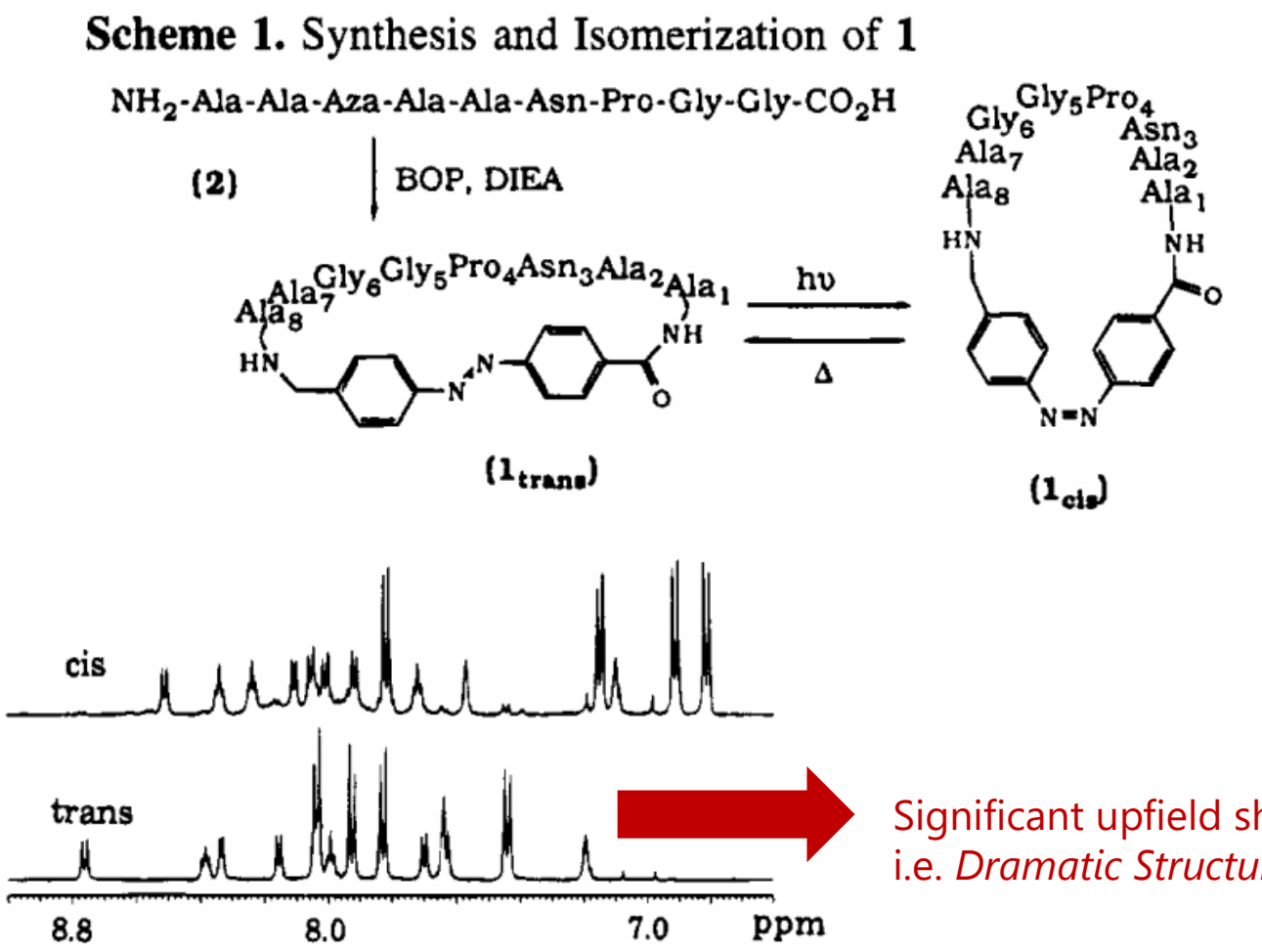

Figure 1. One-dimensional ^{1}H NMR spectra of $\mathbf{1}_{cis}$ and $\mathbf{1}_{trans}$ showing the aromatic/amide portions of the spectra.

J. Chmielewski *et al. J. Am. Chem. Soc.* **1995**, *117*, 8466.

Photomodulation of Redox/Folding of Proteins

Cysteine Motif
(native sequence)

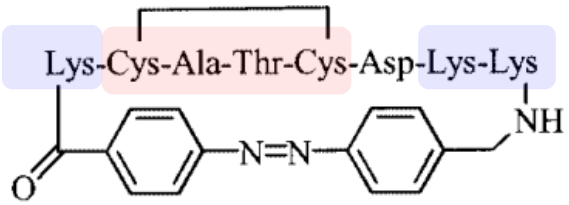

Cyclic bis(cysteinyl)-AMPB peptide

- ✓ Water Soluble (Lys residues)
- ✓ NO oligomers
- ✓ Minimal degradation

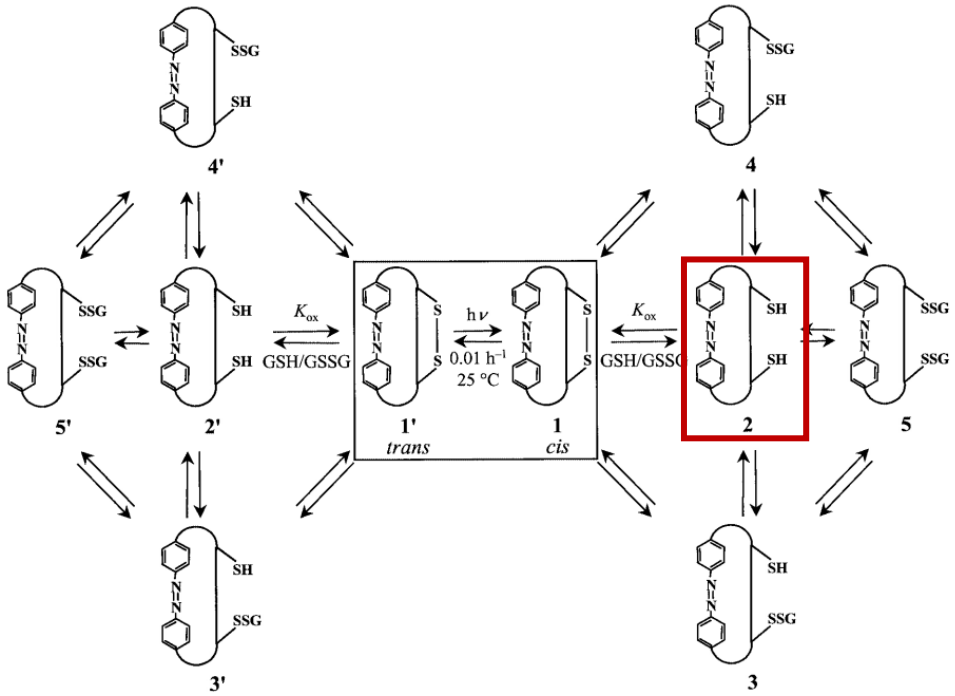

Figure 2. Thiol/disulfide exchange equilibria of the AMPB peptide **1** in the *cis*- and *trans*-azo configuration with the glutathione redox buffer; the species related to the *trans* isomer are indicated with ′

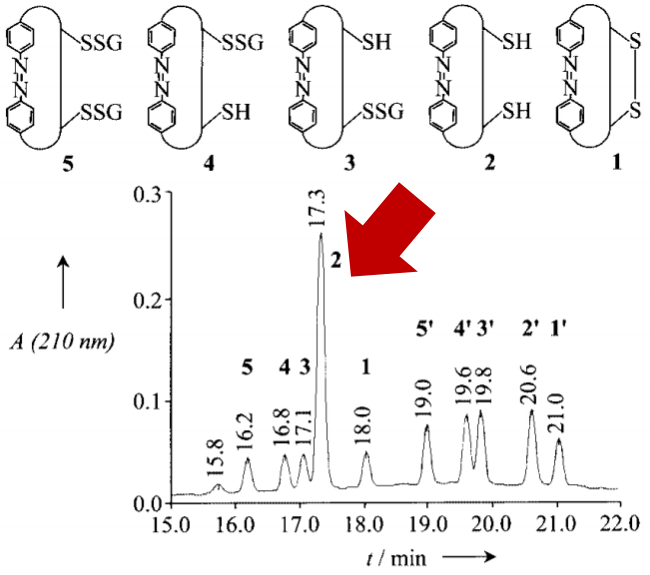

Figure 3. HPLC profile of the mixture of the *cis* and *trans* isomers of the AMPB peptide **1** equilibrated with GSH/GSSG at pH = 7 and 25 °C; the species related to the *trans* isomer are indicated with ′

L. Moroder *et al. Eur. J. Org. Chem.* **2002**, 2144.

Differentiation of Redox Potentials

Table 1. Equilibrium constants of the thiol/disulfide exchange reactions between the AMPB peptide **1** in the *cis*- and *trans*-azo configuration and glutathione; the corresponding redox potentials were calculated with the value of −240 mV for glutathione,[7] at pH = 7 and 25 °C

Azobenzene configuration	K_{ox} [mM]	E_0' [mV]
trans	49 ± 2	−201 ± 1
cis	0.80 ± 0.05	−147 ± 1

trans: high K_{ox} ⇒ exists as disulfide (oxidized form)
cis: low K_{ox} ⇒ exists as thiol (reduced form)

i.e. The cis isomer is **more *oxidizing***

L. Moroder *et al. Eur. J. Org. Chem.* **2002**, 2144.

Catalysis of Oxidative Refolding of Proteins

Table 2. Effect of the AMPB peptide **1** azo configuration and concentration on the refolding of reduced and denatured RNase A (24 μM) at pH = 7.4 and 30 °C; the concentration of GSH was 960 μM in Entries 1−5, and 480 μM in Entries 6−12; the concentration of GSSG was 192 μM in Entries 1−5, 96 μM in Entry 6, 72 μM in Entries 7 and 10, 48 μM in Entries 8 and 11

Entry	RNase A/GSH/GSSG/1	A_{max} [a] [%]	k_{app} [a] [h^{-1}]	Initial rate[b] [pmol min^{-1}]
1	1:40:8:−	77 ± 4	0.14 ± 0.02	2.6 ± 0.4
2	1:40:8:0.5 *trans*	75 ± 2	0.16 ± 0.01	2.9 ± 0.2
3	1:40:8:1 *trans*	85 ± 6	0.15 ± 0.02	2.9 ± 0.4
4	1:40:8:0.5 *cis*	75 ± 5	0.18 ± 0.02	3.2 ± 0.4
5	1:40:8:1 *cis*	86 ± 5	0.16 ± 0.02	3.3 ± 0.5
6	1:20:4:−	64 ± 2	0.072 ± 0.004	1.1 ± 0.1
7	1:20:3:1 *trans*	83 ± 3	0.054 ± 0.003	1.1 ± 0.1
8	1:20:2:2 *trans*	101 ± 4	0.046 ± 0.003	1.1 ± 0.1
9	1:20:−:4 *trans*	50 ± 2	0.13 ± 0.01	1.6 ± 0.1
10	1:20:3:1 *cis*	94 ± 3	0.064 ± 0.004	1.4 ± 0.1
11	1:20:2:2 *cis*	98 ± 4	0.072 ± 0.005	1.7 ± 0.1
12	1:20:−:4 *cis*	72 ± 6	0.12 ± 0.02	2.1 ± 0.4

[a] A_{max} and k_{app} represent the extrapolated maximal activity and the "apparent rate constant" (k_{app}) obtained from the fitting of the experimental curves with the following Equation: % RNase A activity = $A_{max}(1 - e^{-k_{app}t})$. [b] The initial rate was estimated from the first derivative at $t = 0$ of the reactivation curves.

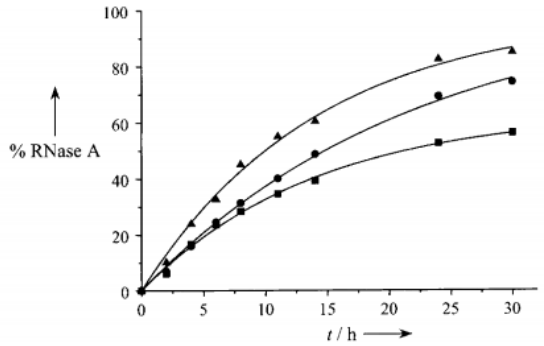

Figure 6. Effect of AMPB peptide **1** on the glutathione-dependent refolding of reduced and denatured RNase A (24 μM) at pH = 7.4 and 30 °C; the following refolding conditions were used: RNase/GSH/GSSG (black squares) 1:20:4; RNase/GSH/GSSG/*trans* isomer (black circles) 1:20:2:2; RNase/GSH/GSSG/*cis* isomer (black triangles) 1:20:2:2

"Remarkable disulfide reshuffling activity"

Positive effect on the initial rate:

cis isomer → observed

trans isomer → NOT observed

⇒ Differentiation of redox potentials

*Both isomers proved to be efficient additives (entry 7,8)

L. Moroder *et al. Eur. J. Org. Chem.* **2002**, 2144.

Strategies for Conformational Control

Backbone incorporation approach

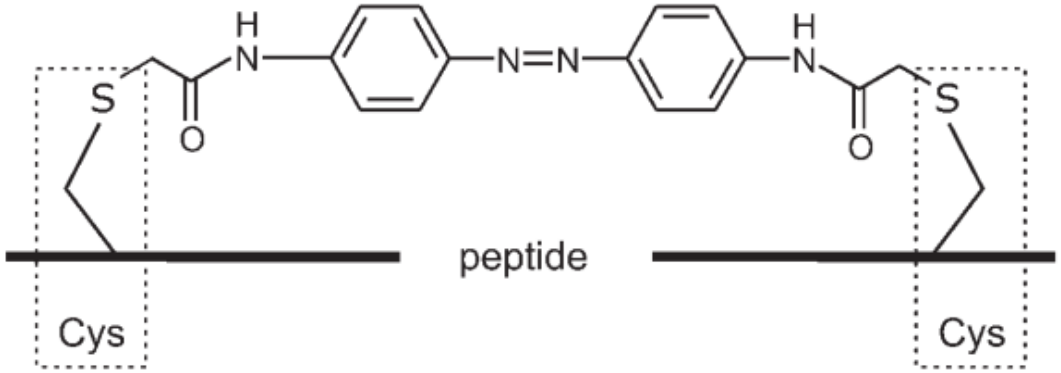

Side-chain Cross-link approach

Images from Scheme 2 of: C. Renner and L. Moroder, *ChemBioChem*. **2006**, *7*, 868.

Example II. Side-chain Cross-link Approach

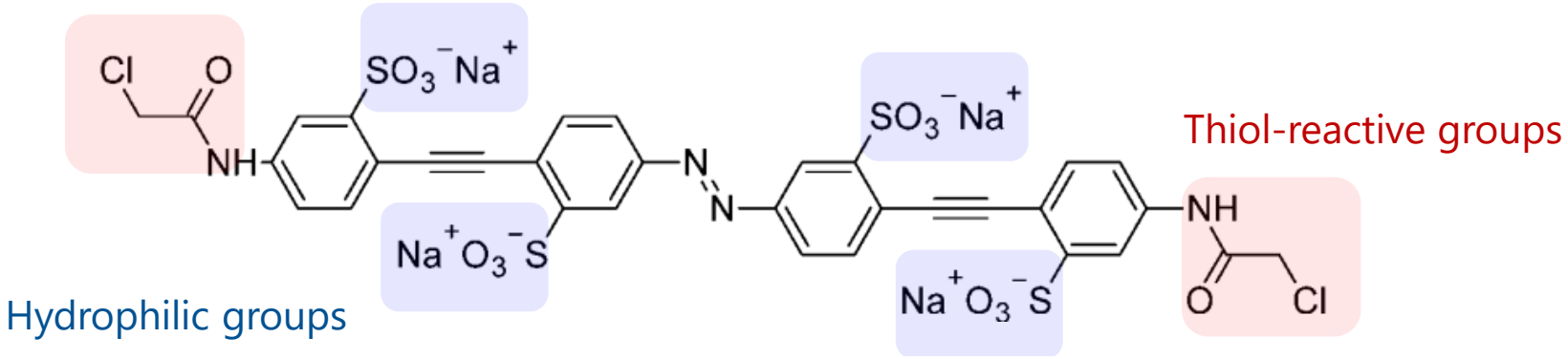

3,3′-diazene-1,2-diylbis{6-[2-sulfonate-4-(chloroacetylamino)phenylethynyl]benzene sulfonic acid} (DDPBA)

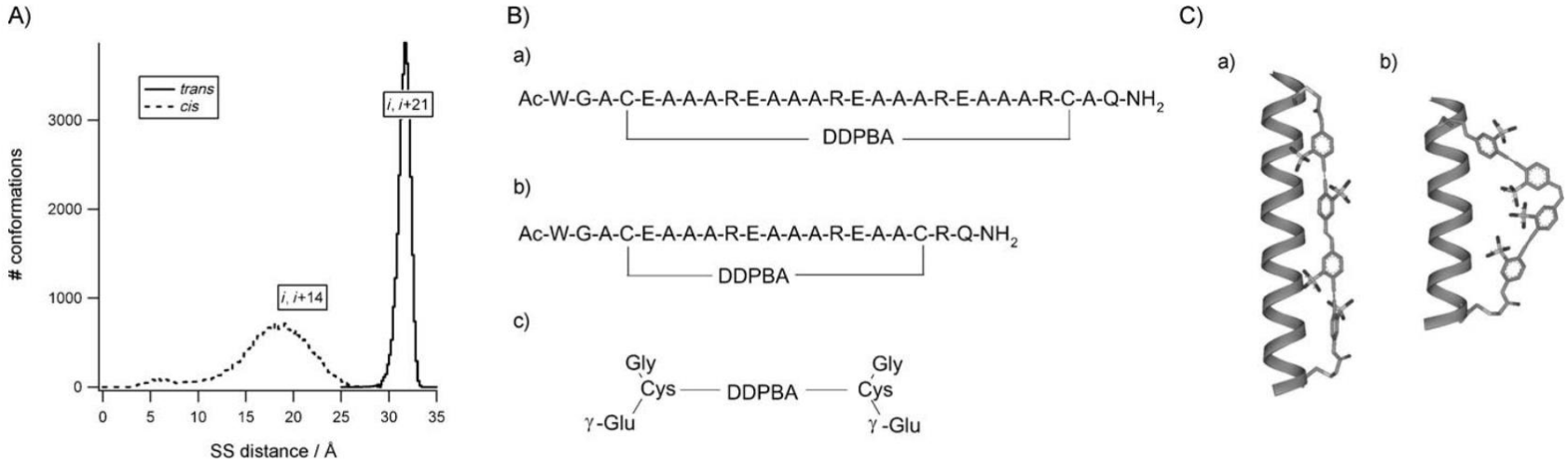

Figure 1. A) Graph of end-to-end distances for *trans* and *cis* forms of DDPBA calculated from molecular dynamics simulations. S–S spacings in ideal helical peptides with Cys residues at *i*, *i*+14 and *i*, *i*+21 are also shown. B) Primary sequences of a) XFZ21, b) XFZ14 and c) XGSH. C) Models of a) *trans* DDPBA-XFZ21 and b) *cis* DDPBA-XFZ14.

A. Woolley *et al*. *ChemBioChem*. **2008**, *9*, 2147.

Effects of Structural/Functional Changes in Peptides

Table 1 Summary of results for effects of cross-linker on peptide conformations (percentages represent helix content)

Conditions		(X)FZ21 (trans-compatible)	(X)FZ14 (cis-compatible)
No irradiation	un-cross-linked (control)	65%	32%
	cross-linked w/ trans DDPBA	41%	20%
irradiation (400 nm)	cross-linked w/ 15% cis DDPBA	decrease	increase

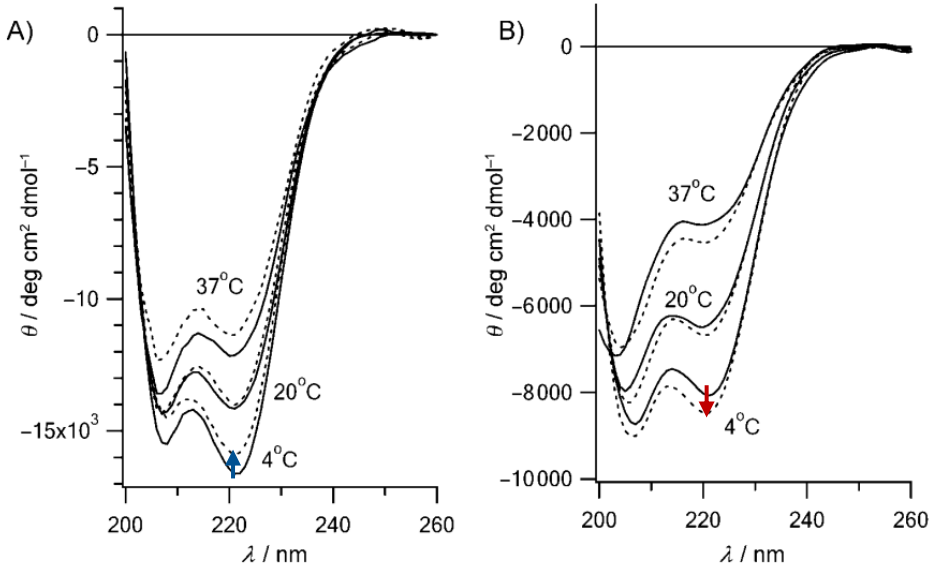

Figure 6. CD spectra of A) XFZ21 and B) XFZ14. Each peptide was scanned at 4, 20 and 37°C. Spectra after dark-adaptation are shown with solid lines. Spectra taken after irradiation (~15% *cis* isomer) are shown with dotted lines. (50 μM peptide in 10 mM phosphate buffer, pH 7.0.)

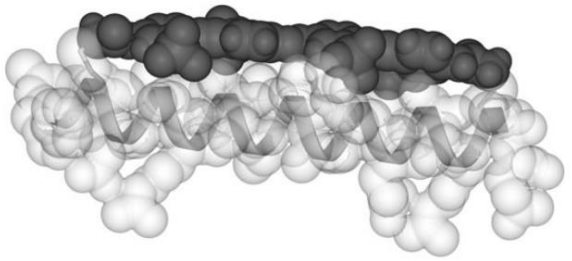

Figure 5. Model of XFZ21 showing close-packing between the DDPBA cross-linker (dark grey) and the peptide (light grey) van der Waals surfaces.

Close packing of cross-linker on peptide surface

→ Distortion of ideal helix geometry (i.e. steric interference)

⇒ **"Lower than expected" helicity**

A. Woolley *et al. ChemBioChem.* **2008**, *9*, 2147.

Bidirectional Photocontrol of Peptides

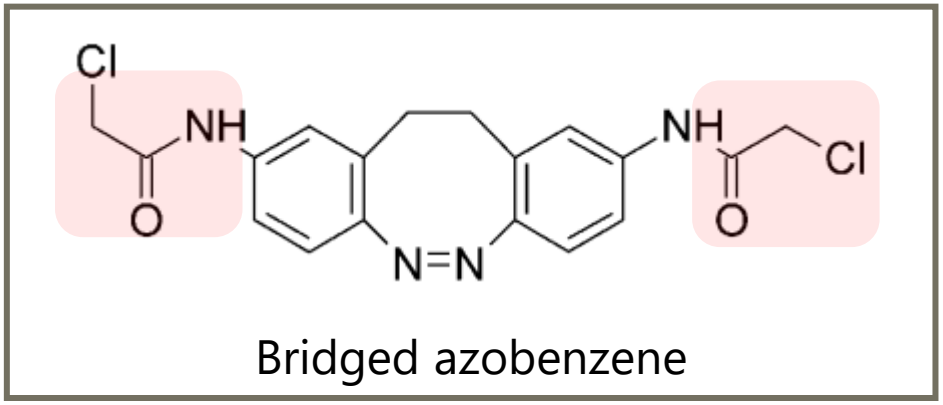

Bridged azobenzene

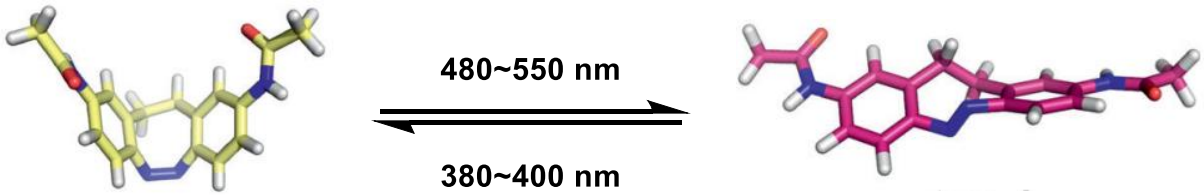

cis

MORE STABLE

trans

- ✓ Severely strained, unstable trans-isomer
- ✓ Photoisomerization efficiency ~100%
- ✓ Large separation of absorption bands (of the cis and trans isomers)
- ✓ Stable against reduction by glutathione

⇒ *Exceptional photoswitching properties!!*

A. Woolley *et al. Angew. Chem. Int. Ed.* **2012**, *51*, 6452.

Multiple Rounds of Photoswitching

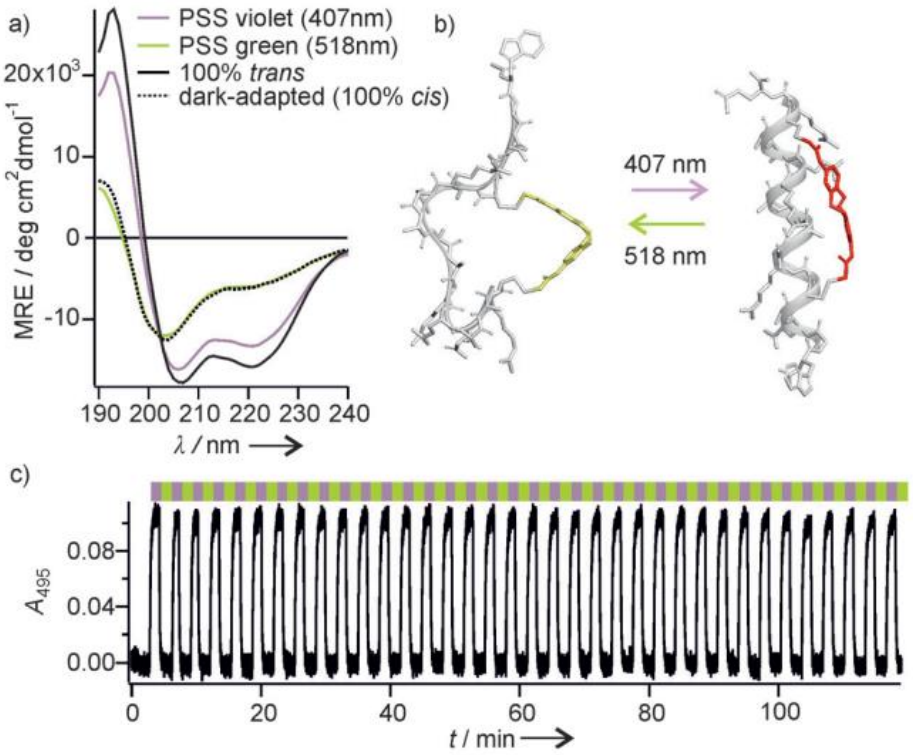

Figure 2. Photoswitching of helical peptide conformation with the bridged azobenzene derivative **3**. a) CD spectra obtained with irradiation conditions shown at 20°C (5 mM Na phosphate buffer, pH 7.0). b) Models showing FK-11 (AcWGEACAREAAAREAACRQ-NH_2) cross-linked with **3** in the *cis* (left) and *trans* (right) conformations. c) Multiple rounds of photoswitching (monitored by the absorbance of the *trans* isomer) can be carried out in the presence of 5 mM reduced glutathione.

A. Woolley *et al. Angew. Chem. Int. Ed.* **2012**, *51*, 6452.

Steric Interactions in Conformational Dynamics

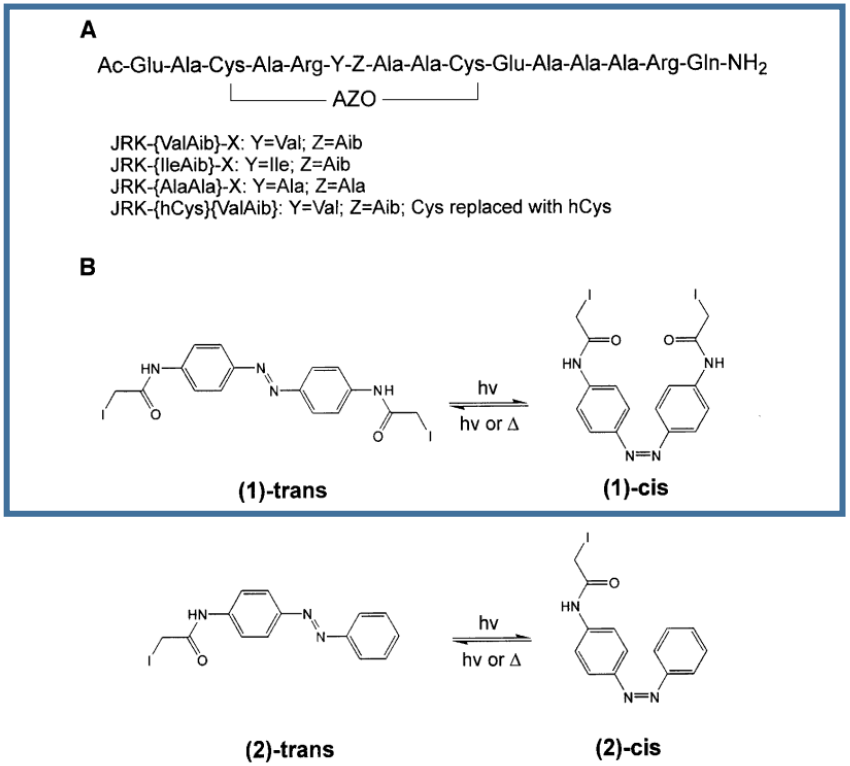

Fig. 1. Structures of peptide variants and azobenzene reagents. (**A**) Primary sequence of the cross-linked peptides. AZO refers to the cross-linker (**1**) after reaction with the two cysteine side chains [or homocysteine (hCys) in JRK-{hCys}{ValAib} (Aib = α-aminoisobutyric acid)]. (**B**) Structures of the azobenzene cross-linker (**1**) and the azobenzene modifying reagent (**2**).

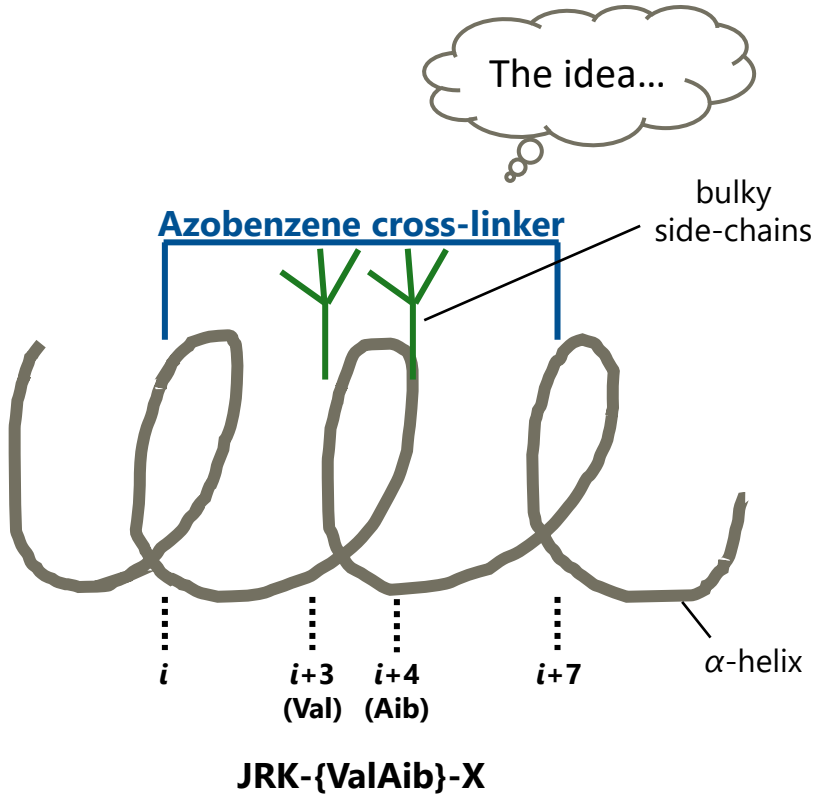

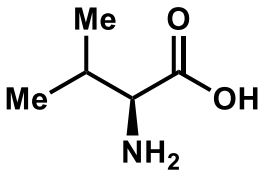

Valine

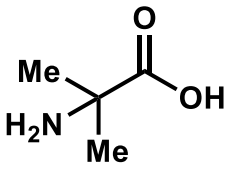

2-Aminoisobutyric acid

Bulky Groups: Ile > Val, Aib > Ala

⇒ Directly interact with trans-azobenzene cross-linker

A. Woolley *et al. Protein Engineering.* **2002**, *15*, 7, 561.

Photoisomerization of Peptide Variants

72% *cis*-azo
characteristic spectra of α-helix

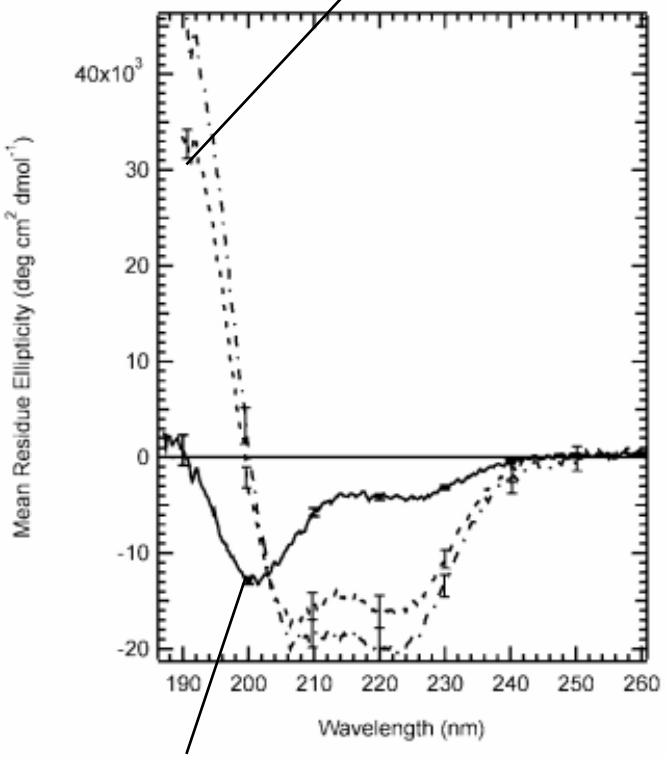

***trans*-azo**
disordered, small degree of helicity

Fig. 3. Effects of photo-irradiation on JRK-{AlaAla}-X. (**A**) CD spectra of dark-adapted (*trans*) JRK-{AlaAla}-X (solid line) [45 μM, 5 mM sodium phosphate buffer (pH 7), 10 ± 1°C] and irradiated JRK-{AlaAla}-X (dotted line) [370 nm light, 3 min, 70 W]. Calculated CD spectrum for 100% *cis* (dashed-dotted line). (**B**) UV spectra of JRK-{AlaAla}-X, dark-adapted (*trans*) (solid line) and irradiated (dotted line). The spectrum of the 100% *cis* form of the cross-linker is shown as a dashed-dotted line.

Table II. Helical content of cross-linked peptides

Peptide	Sample	Corrected $\theta_{222\ nm}$	% Helix[a]
JRK-{ValAib}-X	*Trans*	–3410 ± 200	11
	Cis[b]	–18100 ± 500	60
JRK-{IleAib}-X	*Trans*	–3180 ± 120	11
	Cis	–21100 ± 920	70
JRK-{AlaAla}-X	*Trans*	–4050 ± 330	14
	Cis	–20030 ± 1300	67
JRK-{hCys}{ValAib}-X	*Trans*	–4630	15
	Cis	–16534	55
JRK-{ValAib}-Mod	*Trans*	–17672	59
	Cis	–16200	54

All CD measurements were performed at 10 ± 1°C with peptide concentrations from 40 to 70 μM in 5 mM $NaPO_4$ (pH 7.0). Mean residue ellipticity ($\theta_{222\ nm}$) is reported in degrees/cm^2.$dmol^{-1}$. Each value represents the average of three individual experiments (five scans each), with the exception of JRK-{hCys}{ValAib}-X and JRK-{ValAib}-Mod, which were single samples with five scans averaged.
[a]Calculated by using $(\theta_{222\ nm})/\{-40\ 000[(n-4)/n]\}\times 100\%$. Estimated 95% confidence limits ±1% for dark-adapted and ±5% for irradiated data.
[b]Values for *cis* forms of the peptide were obtained by correcting observed CD spectra for the % *cis* form present as determined by UV (see Materials and methods).

.. Woolley *et al. Protein Engineering.* **2002**, *15*, 7, 561.

Molecular Modelling

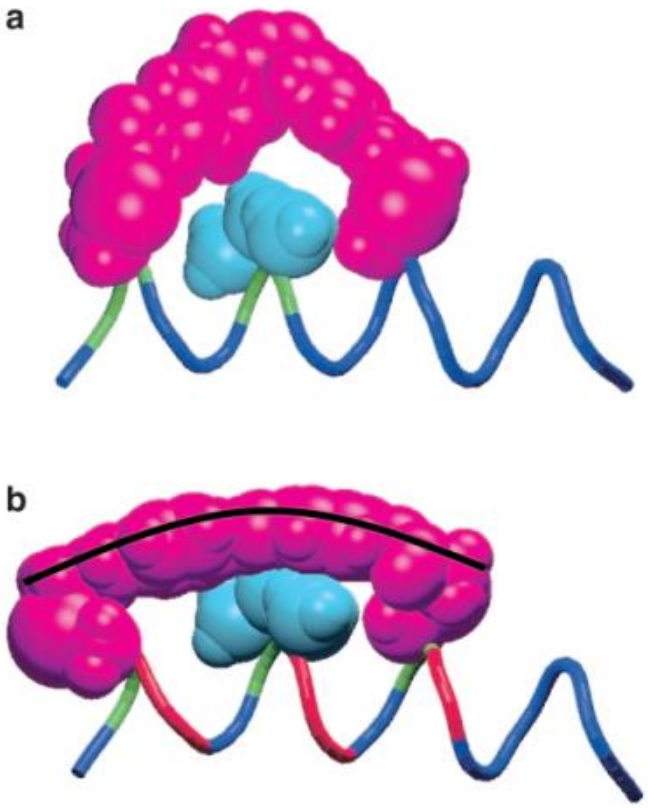

Fig. 4. Energy optimized molecular models of JRK-{ValAib}-X. Models with the cross-linker in the *cis* form (**a**) and the *trans* form (**b**). Space filling representations of the cross-linker and Cys side chains, from Cb, are coloured violet. In cyan are the extra atoms of the amino acid side chains for Val and Aib compared with Ala and Ala. The peptide backbone is shown as a tube with colours assigned in accordance with the strength of the α-helical hydrogen bonds made on a residue by residue basis: blue = strong, green = intermediate, red = weak. A thick black line shows the deviation from planarity of the *trans* isomer required for it to accommodate an α-helical peptide backbone conformation. Figure prepared using VMD (Humphrey *et al.*, 1996) and Raster3D (Merritt and Bacon, 1997).

cis → *trans* photoisomerization

↓

Weakening of helical hydrogen bonds

↓

Distortion from ideal α-helical geometry

↓

Altering the underlying residues from:

JRK-{AlaAla}-X ⇒ JRK-{ValAib}-X or JRK-{IleAib}-X

(small) (bulky)

"*marginally* increases disruption of helicity"

A. Woolley *et al. Protein Engineering.* **2002**, *15*, 7, 561.

Azobenzenes

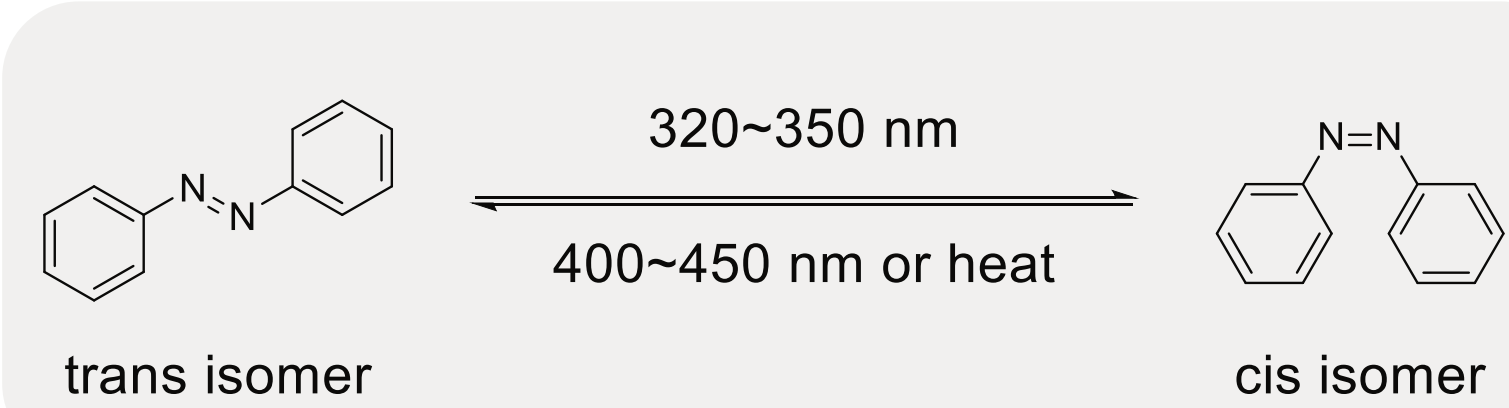

Great use in remote control of biological structures/funtions using light!!

Table of Contents

Summary

- ✓ Azobenzenes are versatile photoswitches in biomolecules
- ✓ Photoisomerization induces the “end-to-end distance change” essential for photomodulation of biological structures/functions
- ✓ Steric interactions are not crucial for conformational dynamics
- ✓ Azobenzene architecture may be applicable to photooxygenation catalysts??

Thank you for your attention.

Supplementary Slides

Absorption Spectra of Azobenzenes

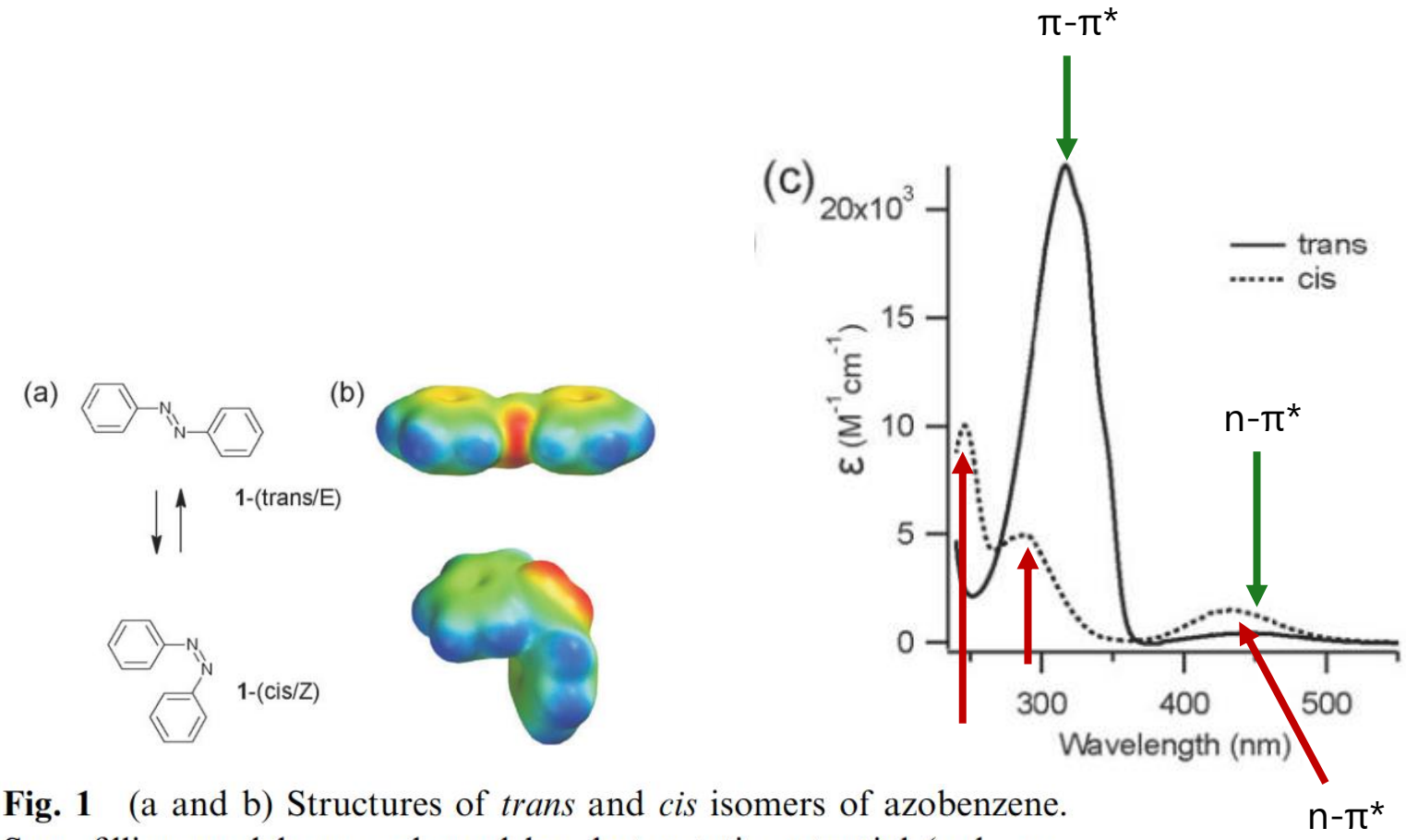

Fig. 1 (a and b) Structures of *trans* and *cis* isomers of azobenzene. Spacefilling models are coloured by electrostatic potential (red—negative to blue—positive). (c) Electronic absorption spectra of the *trans* and *cis* isomers of azobenzene dissolved in ethanol.

A. Woolley *et al. Chem. Soc. Rev.* **2011**, *40*, 4422.

Absorption Spectra of Azobenzenes

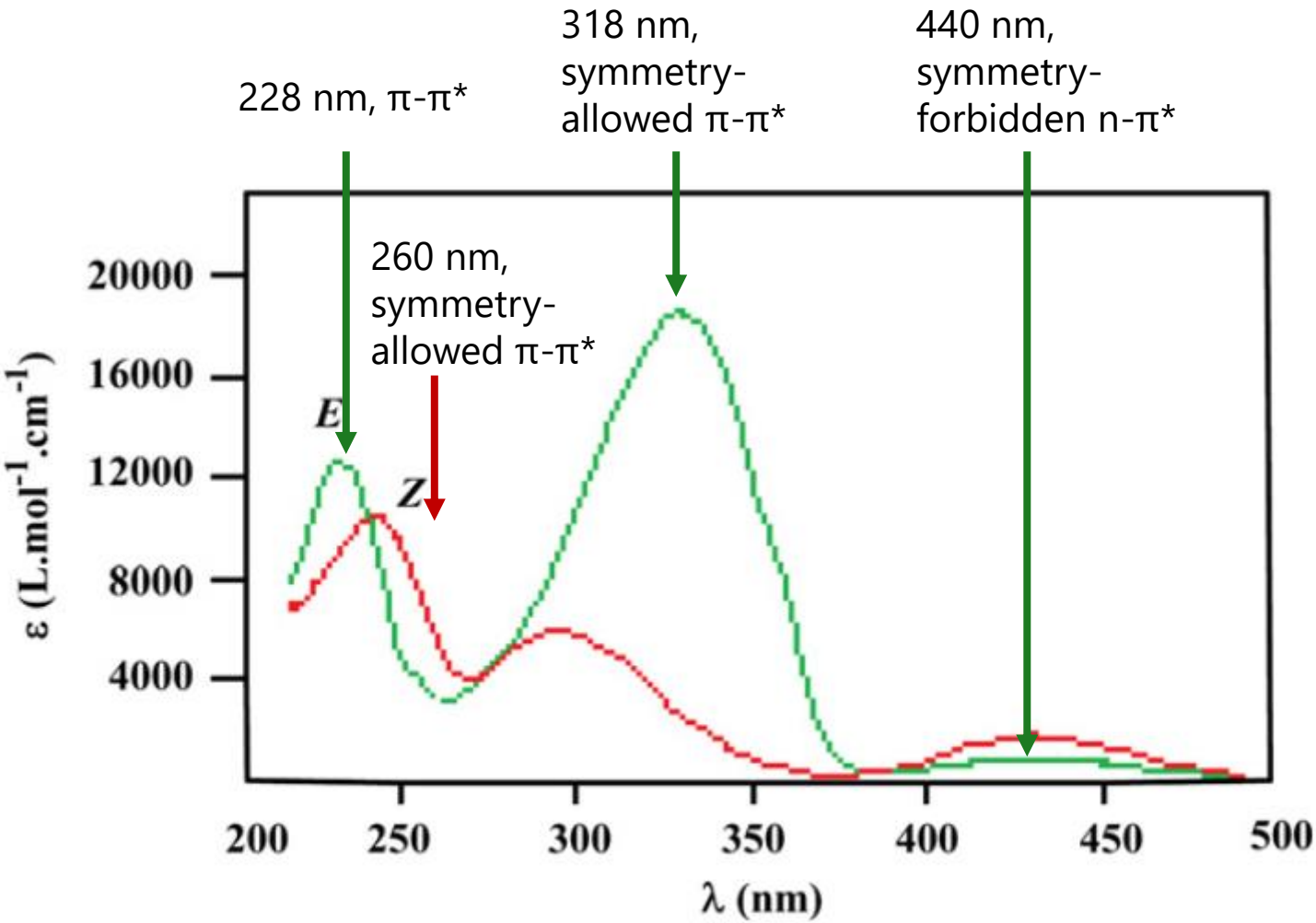

Figure 4. UV–vis absorption spectra of *E*- and *Z*-azobenzene in ethanol.

C. Len *et al. Tetrahedron*, **2009**, *65*, 10105.

Spectral Tuning

Donor aniline

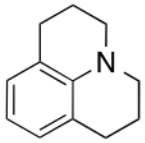

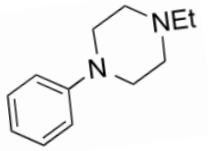

Table 2
Photophysical data for donor–acceptor azobenzenes **3** and **5**.

Dye	Substituent (R^1)	σ for R^1		λ_{max} [nm][a]	$\varepsilon \times 10^{-3}$[L mol^{-1} cm^{-1}][a]
		σ_p	σ_m		
3a	4-NO_2	+0.81	–	513	25
3b	4-CN	+0.66	–	487	31
3c	4-CF_3	+0.54	–	466	22
3d	4-CO_2CH_3	+0.46	–	474	26
3e	3,5-$(NO_2)_2$	–	+0.71	513	42
3f	3,5-$(CF_3)_2$	–	+0.49	486	26
3g	3,5-$(CO_2CH_3)_2$	–	+0.36	471	26
5a	4-NO_2	+0.81	–	448	26
5b	4-CN	+0.66	–	428	26
5c	4-CF_3	+0.54	–	414	23
5d	4-CO_2CH_3	+0.46	–	419	25
5e	3,5-$(NO_2)_2$	–	+0.71	454	28
5f	3,5-$(CF_3)_2$	–	+0.49	427	22
5g	3,5-$(CO_2CH_3)_2$	–	+0.36	416	21

[a] Measured in AcOEt (10^{-5} mol L^{-1}).

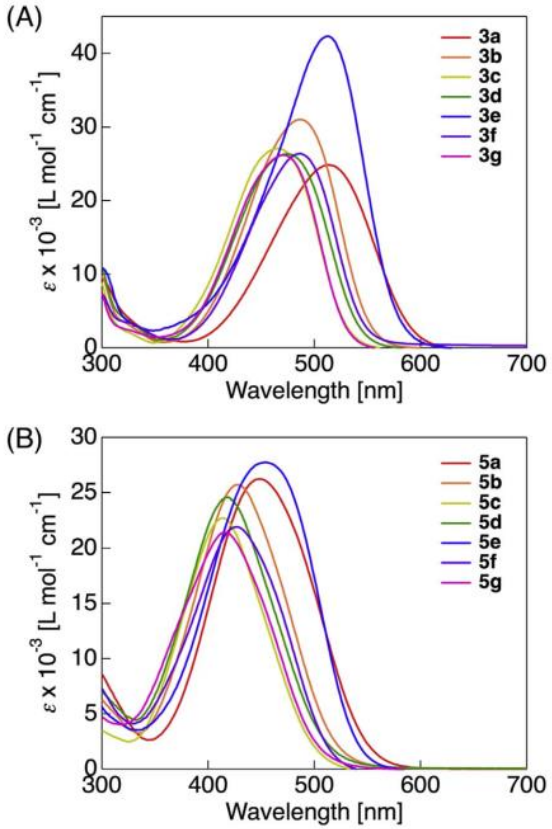

Fig. 2. Absorption spectra of donor–acceptor azobenzenes in AcOEt (10^{-5} mol L^{-1}) at room temperature.
(A) **3a–g**, (B) **5a–g**.

⇒ Donor-Acceptor abilities and substituents on the rings strongly influence the position/shapes of absorption bands

O. Tsutsumi *et al. Dyes and Pigments.* **2018**, *150*, 89.

Circular Dichroism Spectra

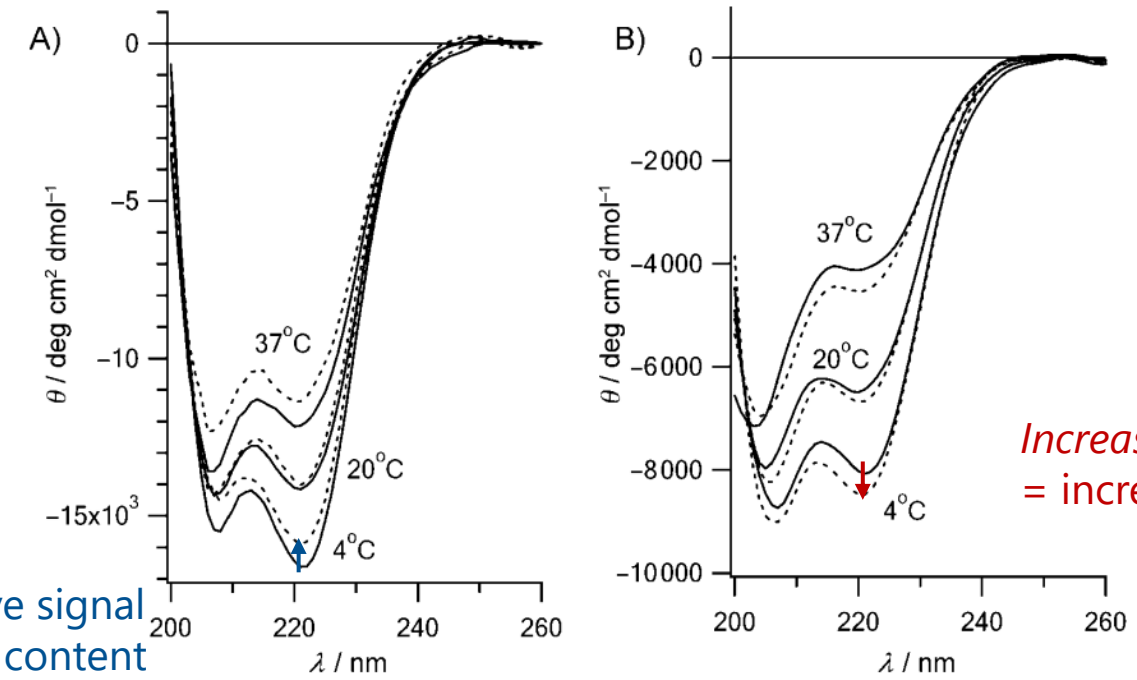

Decrease in negative signal
= decrease in helix content

Increase in negative signal
= increase in helix content

Figure 6. CD spectra of A) XFZ21 and B) XFZ14. Each peptide was scanned at 4, 20 and 37°C. Spectra after dark-adaptation are shown with solid lines. Spectra taken after irradiation (~15% *cis* isomer) are shown with dotted lines. (50 μM peptide in 10 mM phosphate buffer, pH 7.0.)

A. Woolley *et al*. *ChemBioChem*. **2008**, *9*, 2147.

Application of Azobenzenes

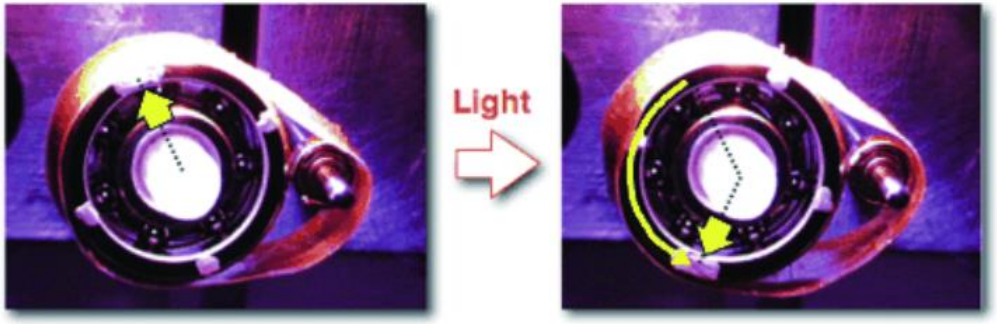

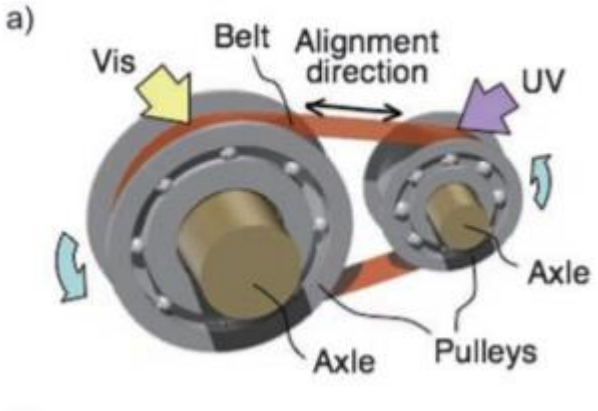

T. Ikeda *et al*. *Angew. Chem. Int. Ed.*, **2008**, *47*, 27, 4986.

要約

東京工業大学　資源化学研究所の池田富樹教授のグループは，光に反応して変形し力を出す高分子材料（「光運動材料」）を開発，単位断面あたりに発生できる力を増し，実際に光を照射すると回転する光モーター（図1）の試作に成功した．

この光モーターには，アゾベンゼンという色素を高分子側鎖に導入した液晶エラストマー・フィルムが使われている．この材料は紫外線を照射すると縮み，可視光を照射すると伸びる性質がある．これをベルト状にして2つの軸にかけ，2つの場所に紫外線・可視光の異なる光を当てると，伸縮によって回転運動が起きる．実験では15秒に1回転程度の回転運動を起こすことができた．

http://www.hyoka.koho.titech.ac.jp/eprd/recently/research/109.html

Photoisomerizable Intramolecular Cross-Linkers

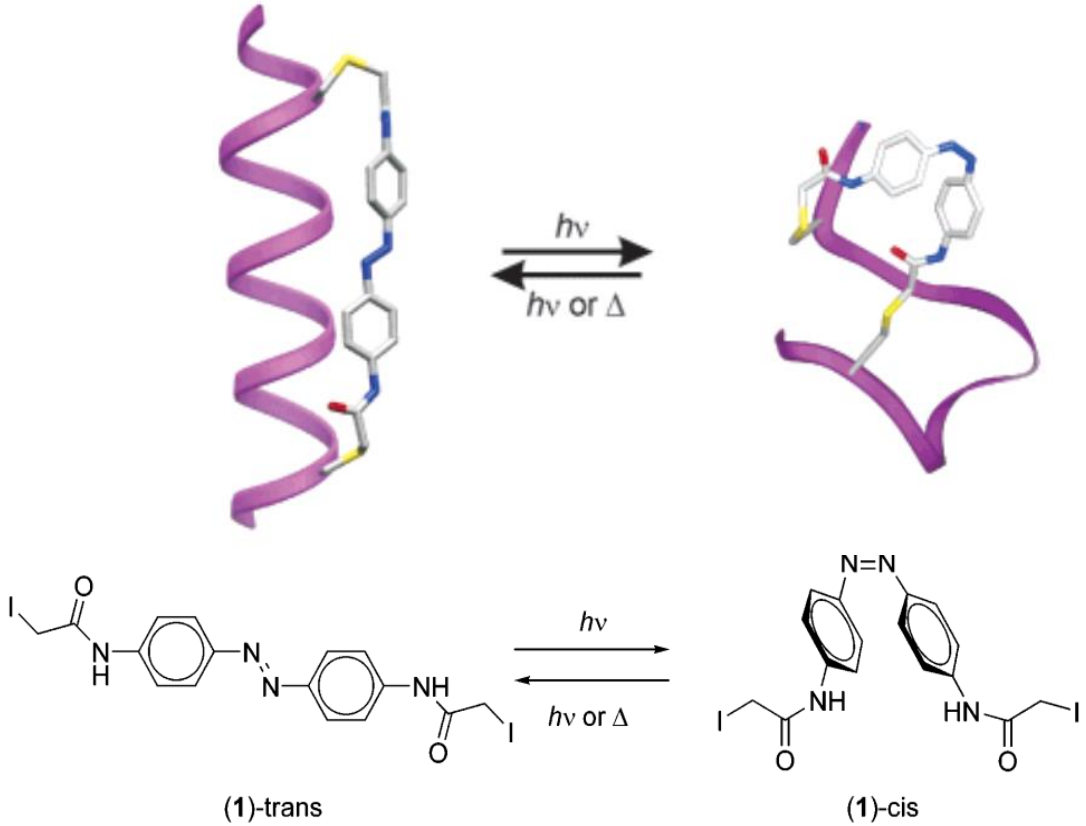

- ✓ α-helical peptide cross-linked between Cys residues (spaced *i*, *i*+11)
- ✓ trans→cis photoisomerization induced decrease in helix content
- ✓ thermal/photoisomerization from cis→trans returns peptide to original helical form

A. Woolley *et al. Acc. Chem. Res.*, **2005**, *38*, 486.

Azobenzene and Aβ

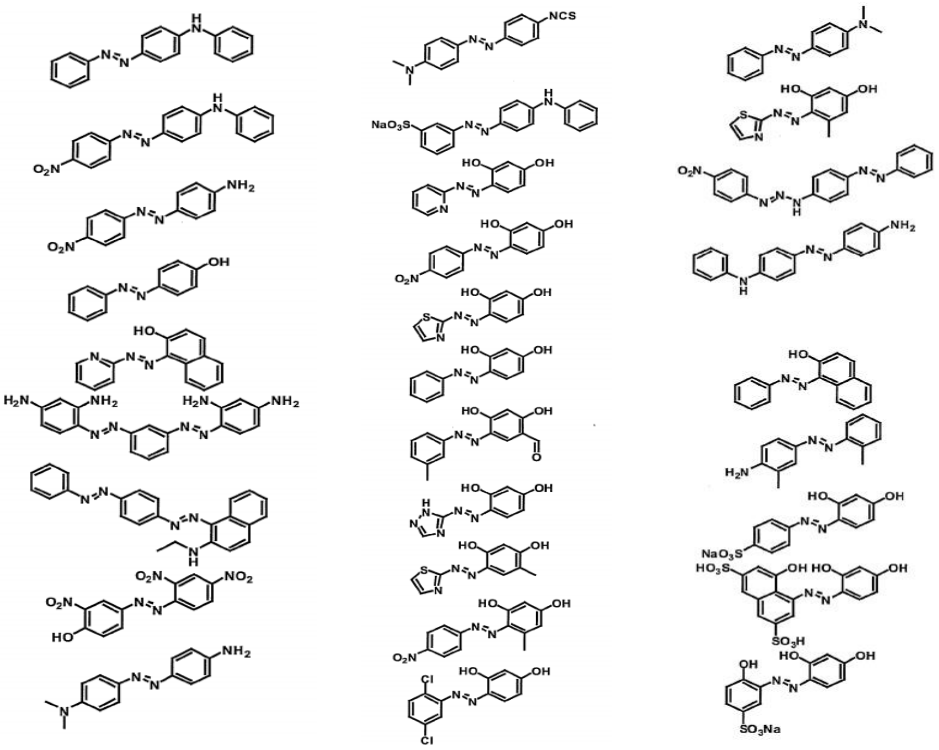

- ✓ Reported to reduce Aβ-monomer and dimer formation in vivo (cell-based assay)
- ✓ Inhibitor of Aβ aggregate formation
- ✓ Modulator of amyloid surface properties
- ✓ Activator of degradation/reduction of Aβ aggregates
- ✓ Suitable for medical applications e.g.) human/veterinary medicine
- ✓ Targets diseases including familial amyloid polyneuropathy (TTR)

E. Wanker *et al.*, inventors; Azo compounds reducing formation and toxicity of amyloid beta aggregation intermediates. European patent EP 2 368 558 A1. 2011.

Geometry and Affinity

Scheme 2. Isomerization of *Z,Z*-5 to *E,E*-5

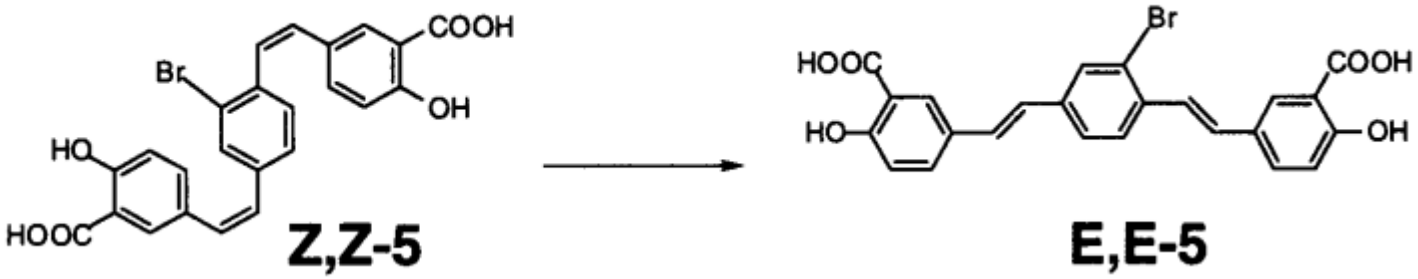

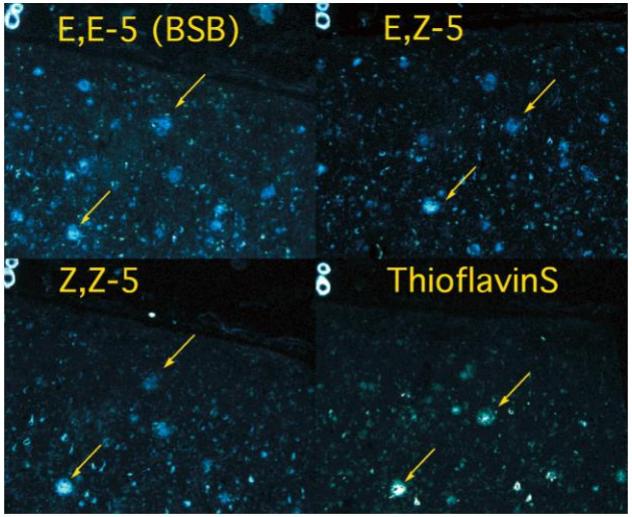

Figure 1. Fluorescent images of *E,E*-5, *E,Z*-5, *Z,Z*-5, and Thioflavin S using adjacent sections of postmortem AD brain. All of the images were obtained under similar incubating conditions using a concentration of 0.05 mM. The vascular amyloid plaques at the upper left-hand corner of each picture were used as markers to align the images.

- ✓ All isomers showed similar binding affinities toward Aβ aggregates
- ✓ Relative distance between the 2 negative charges are unlikely to be the same

⇒ binding affinity to the β-sheet structure may not be due to electrostatic interaction…?

H. Kung *et al. J. Med. Chem.* **2001**, *44*, 2270.

Photoisomerization and Aggregation

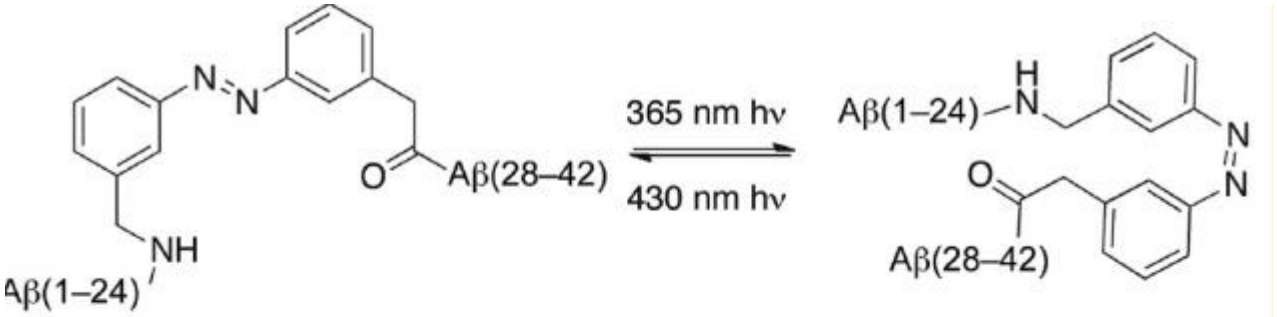

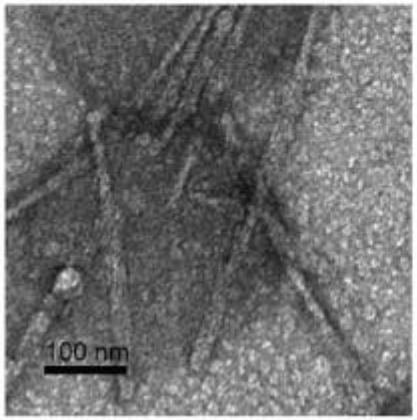

cross-β, native-like fibrils

trans, toxic

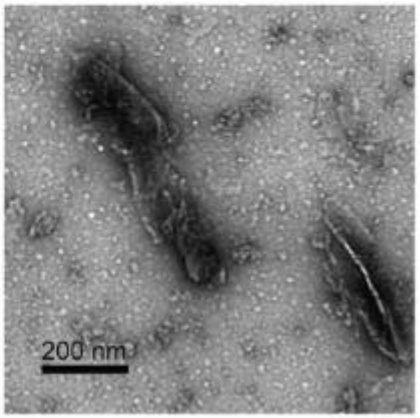

amorphous, non-amyloid aggregates

cis, NOT toxic

L. Nilsson *et al. ACS Neurosci.* **2012**, *3*, 211.

Singlet Oxygen Formation: Mechanism

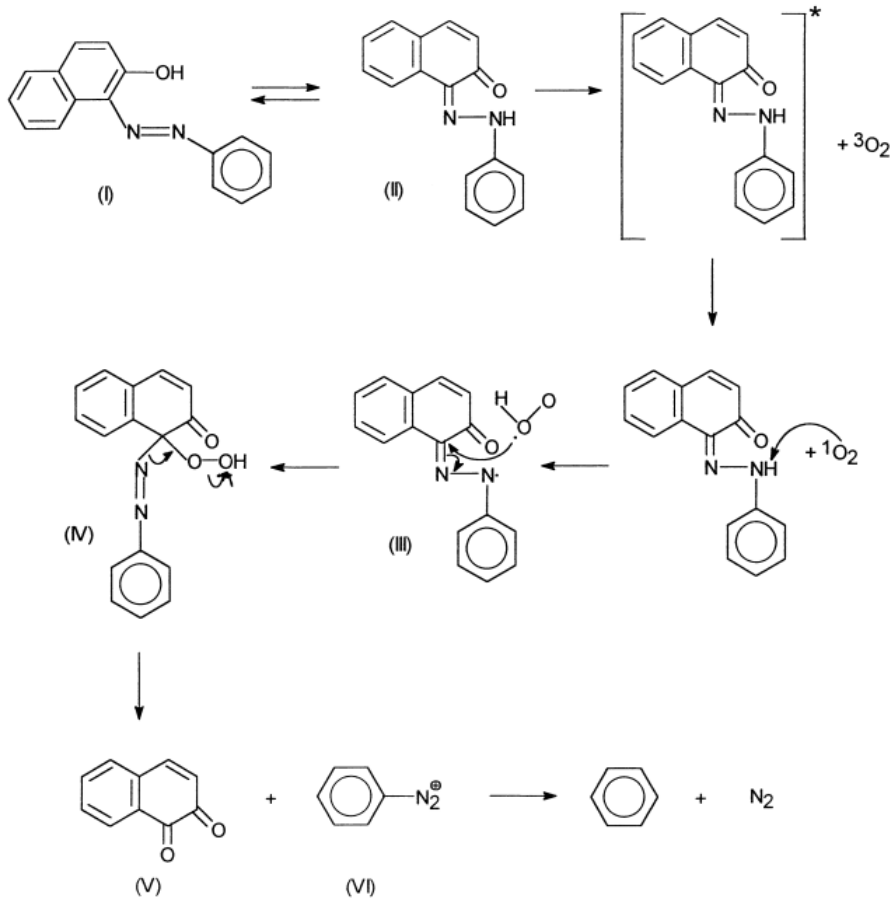

Fig. 1. Self sensitized photo-oxidation of an 1-arylazo-2-naphthol dye via a singlet oxygen type II mechanism.

- ✓ Type II singlet oxygen mechanism
- ✓ Formation of singlet oxygen via energy transfer from *hydrazone tautomer*

D. Worrall *et al. J. Photochem. Photobio. A: Chem.*, **1999**, *125*, 99.

Generation of Singlet Oxygen

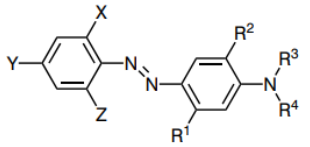

Dye	X	Y	Z	R^1	R^2	R^3	R^4
1	H	H	H	H	H	C_2H_5	C_2H_5
2	H	H	H	H	H	C_2H_5	C_2H_4CN
3	H	H	H	H	H	C_2H_4CN	C_2H_4CN
4	H	NO_2	H	H	H	C_2H_5	C_2H_5
5	H	Br	H	H	H	C_2H_5	C_2H_5
6	NO_2	NO_2	Br	H	H	C_2H_5	C_2H_5
7	Cl	NO_2	Br	H	H	C_2H_5	C_2H_5
8	NO_2	NO_2	Br	$NHCOCH_3$	OCH_3	C_2H_4OH	C_2H_4OH
9	NO_2	NO_2	Cl	$NHCOCH_3$	OCH_3	C_2H_4OH	C_2H_4OH

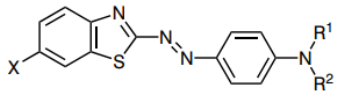

Dye	X	R^1	R^2
10	H	C_2H_5	C_2H_5
11	OCH_3	C_2H_5	C_2H_5
12	NO_2	C_2H_5	C_2H_5

Table 1 Degradation of TPC and dyes **1–12**, and the shift in maximum wavelength ($\Delta\lambda_{max}$) after 4 h irradiation in the Xenotest

	Fading of dyes (%)					
Dye	No additive	DABCO	Sensitiser[a]	$\Delta\lambda_{max}$ (nm)	TPC fading[b]	Light fastness
1	2.5	0	21.0	19	Moderate	4–5
2	1.0	0	16.0	18	Moderate	4–5
3	0	0	14.0	0	Complete	4–5
4	2.2	1	19.5	25	Complete	3–4
5	1.6	0	22.5	38	Complete	5–6
6	3.4	0	25.0	29	Strong	4–5
7	3.7	0	20.0	32	Strong	5–6
8	2.3	0	5.8	0	Complete	6
9	3.4	0	5.3	0	Complete	6–7
10	1.5	0	15.9	12	Complete	2
11	1.0	0	11.0	13	Strong	2
12	2.5	0	6.6	0	Complete	6

a Dyes **1–7**,**10–12** sensitised with Methylene Blue; dyes **8** and **9** sensitised with Fluorescein
b Estimated visually

- ✓ Irradiation with visible light in the presence of air produces singlet oxygen (for all dyes 1~12)
- ✓ Sterically hindered azobenzenes and nitro-substituted heterocyclic azo dyes exhibit very high photostability in the presence of singlet oxygen sensitisers (Methylene Blue, Fluorescein)

J. Sokolowska *et al. J. Photochem. Color. Technol.*, **2003**, *119*, 341.

Generation of Singlet Oxygen

Substituted *trans*-4-NN-dialkylamino-4′-nitroazobenzenes

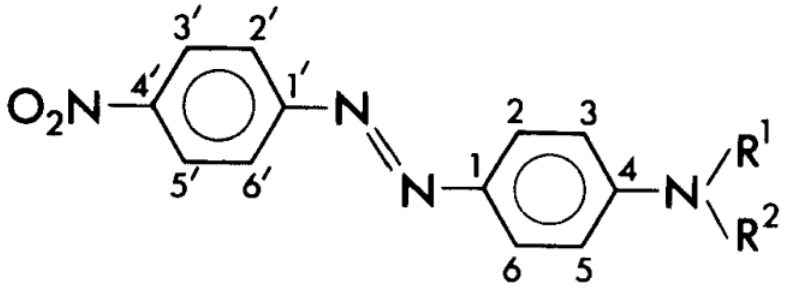

Compound [a]	Position of Substitution 3	6	2′	6′
1	OCH_3	$NHCOCH_3$	Br	NO_2
2	OCH_3	$NHCOCH_3$	Br	CN
3	OCH_3	$NHCOCH_3$	Cl	NO_2
4	OCH_3	$NHCOCH_3$	H	NO_2

(a) R^1 represents the group CH_2CH_2OH; R^2 the group CH_2CH_2CN

- ✓ Irradiation with visible light to 4-*N*,*N*-dialkylamino-4′-nitroazobenzenes, NOT subject to azo-hydrazone-tauotmerism leads to conversion of triplet oxygen to singlet oxygen

D. Schulte-Frohlinde *et al. J. S. D.S.*, **1981**, *97*, 430.

Potential Obstacles for *in vivo* Application

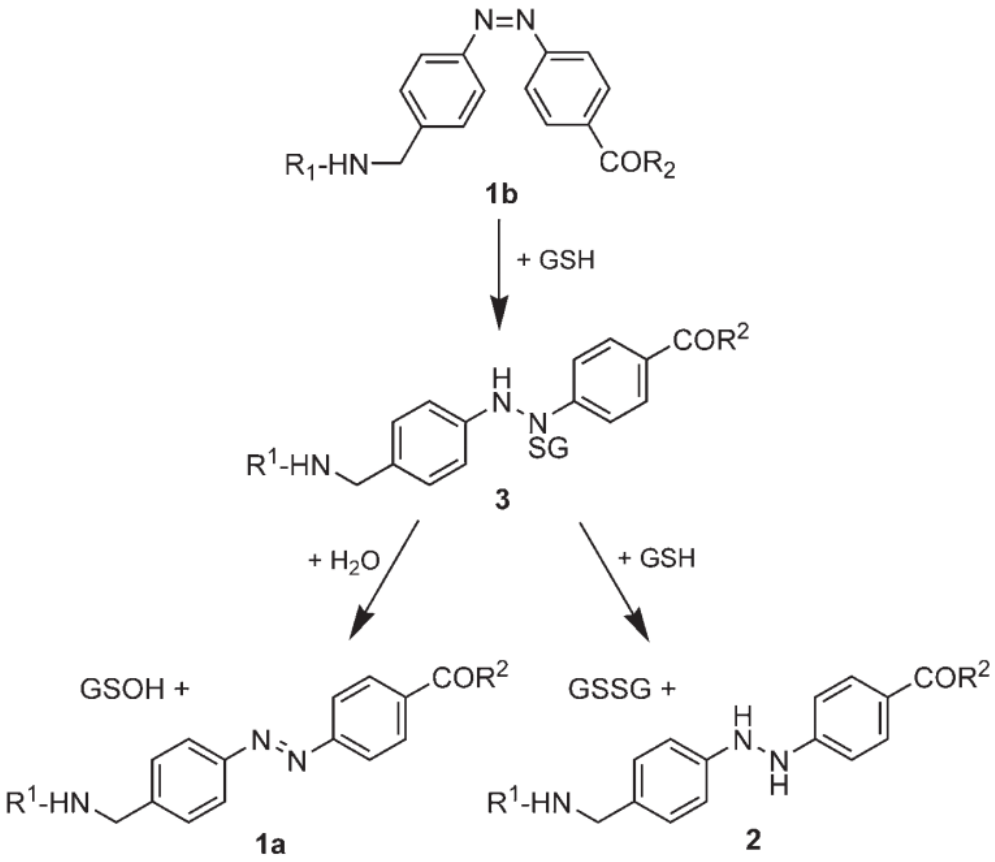

Scheme 2. Proposed mechanism of reduction and *Z*/*E* isomerization of the azobenzene-peptide **1 b** by glutathione. The sulfenic acid that is formed by hydrolysis of the sulfenohydrazide intermediate **3** disproportionates to yield thiol and sulfenic acid.[20]

L. Moroder *et al*. *ChemBioChem*. **2007**, *8*, 591.

Synthesis of Azobenzenes

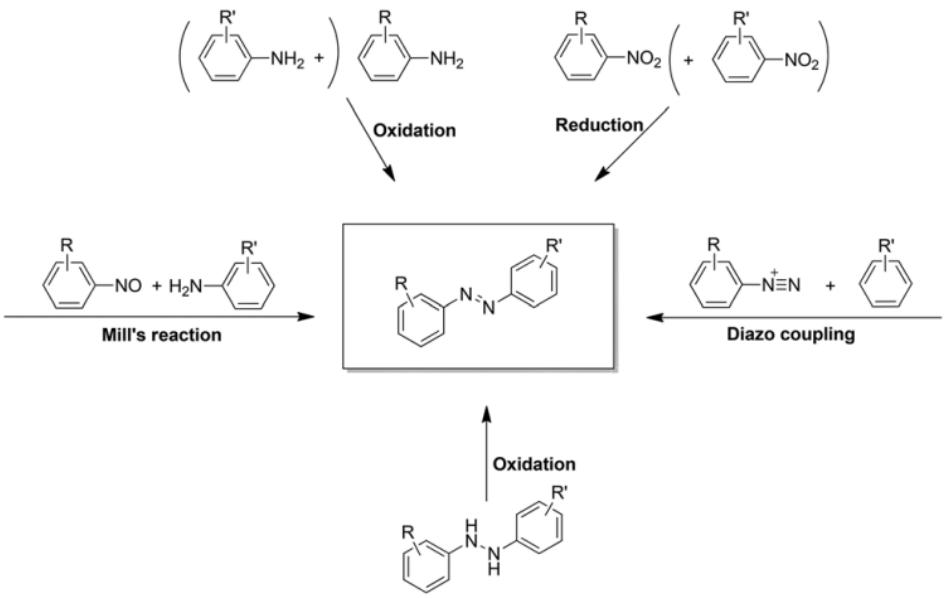

Fig. 3 Synthetic methods of azobenzene derivatives.

Others:

- ✓ Azo coupling reaction
- ✓ Mills reaction
- ✓ Wallach reaction
- ✓ Reduction of azoxybenzenes
- ✓ Reductive coupling of aromatic nitro derivatives
- ✓ Oxidation of anilines
- ✓ Dehydrogenation of arylhydrazines
- ✓ Dimerization reaction of diazonium salts
- ✓ Triazene rearrangement
- ✓ Thermolysis of azides
- ✓ Decomposition of *N*,*N*-'*p*-benzoquinonediimines dioxides
- ✓ Reaction of arylcalcium derivatives with nitrous oxide
- ✓ Metal catalyzed coupling of arylhydrazines
- ✓ Opening of benzotriazoles
- ✓ Reaction of quinones with arylhydrazines
- ✓ Reaction of quinone acetals with arylhydrazines

H. Zhou *et al. Org. Biomol. Chem.* **2018**, *16*, 8434.
E. Merino *et al. Chem. Soc. Rev.* **2011**, *40*, 3835.

Reaction Mechanisms

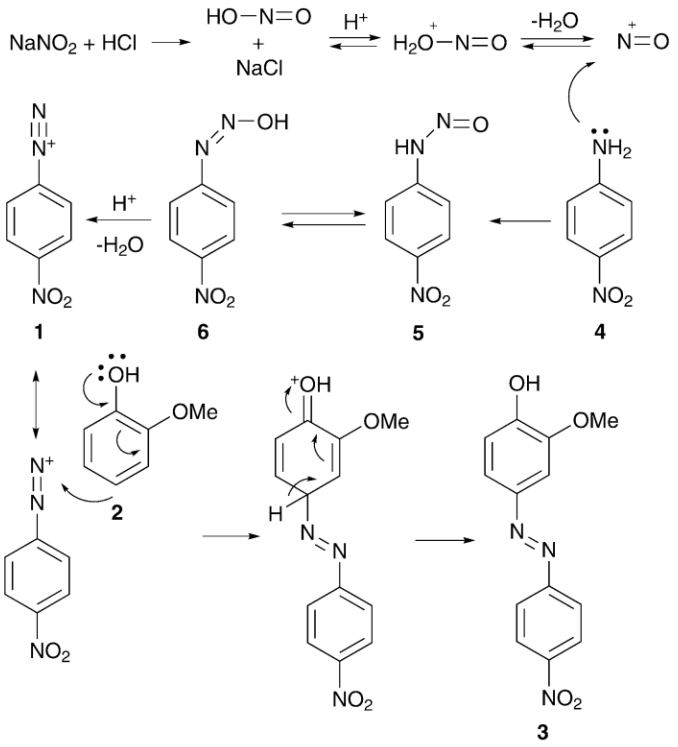

Scheme 2

Diazo coupling reaction

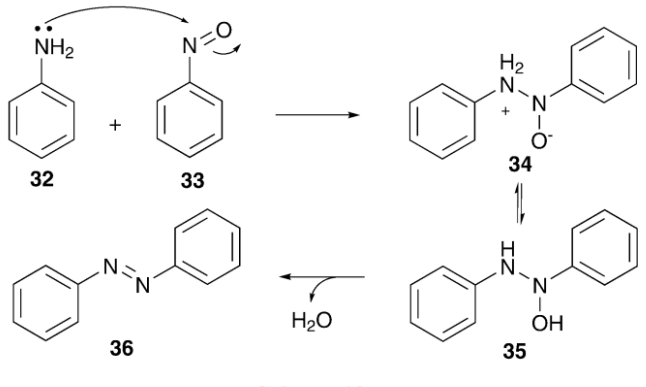

Scheme 10

Mills reaction

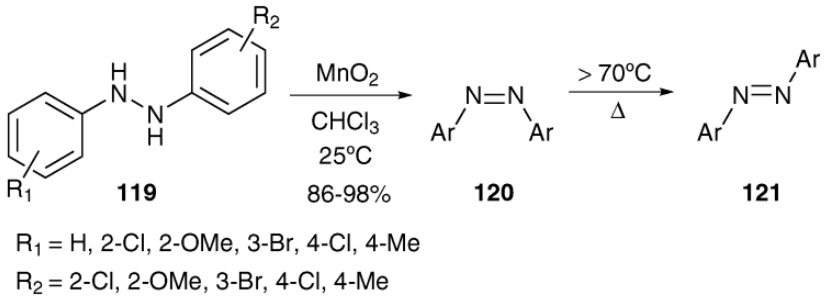

Scheme 37

Oxidation of anilines

E. Merino *et al. Chem. Soc. Rev.* **2011**, *40*, 3835.